To the Editorial Board of *Solid Earth*

Dear Editor and Reviewers:

First of all, we would like to express our sincere gratitude for the huge amount of work that was done by both reviewers. We very much appreciate their careful consideration of our manuscript. The comments were rigorous, but very constructive and friendly. Not only were the recommendations and advice useful for us in the context of the present work, but such comments will also be valuable for our future papers.

We have considered very carefully all the comments of the reviewers, and for the vast majority of the comments, we have made corresponding corrections in the manuscript. Among the most important changes, we can single out the following revisions:

1. We have considerably changed the structure of the main sections in the paper and reformatted the text correspondingly.
2. We have added a test with synthetic Moho.
3. We have added Fig. 3 with travel times versus distance.
4. In Fig. 2, we have added a plot showing the general distribution of all stations of the ENSN.

All the changes are described in detail in the attached response letter.

We hope that you will find our paper improved and suitable for further consideration in *Solid Earth*.

Sincerely yours,

Sami El Khrepy, on behalf of the coauthors

Response letter for the paper by El Khrepy et al. "Seismic structure beneath the Gulf of Aqaba and adjacent areas based on the tomographic inversion of regional earthquake data"

The author's responses are highlighted with violet and indicated with "REP"

Anonymous Referee #1

Summary:

The paper describes a joint inversion of local earthquake travel times for the P- and S-wave velocities and hypocentral locations, and a subsequent interpretation of the results. The paper is generally well-written though a language review of a native English speaker is needed to improve the readability of the text. The paper would also benefit from a reorganization of some of the sections, e.g. the introduction is in my view a mix of a background/motivation for the study with a geologic/tectonic setting. Though the methodology and data selection procedures etc. are fairly clearly explained, there are some aspects here that in my view are missing, and this is in fact where I have my main difficulties with the presented work (point 1-7 below). Otherwise the content is within the scope of SE, and contains potentially interesting material. I am not really familiar with the study area, so I am not familiar with the state of knowledge of the area. I hope a different reviewer is as I might easily have missed something.

Data selection:

1) Data appears to come from two sources – ENSN (the Egyptian National Seismic Network) and ISC (the International Seismological Centre). The authors claim they combine data from (the two?) different catalogues, but they do not say how (Line 121). This seems like a good idea as the ENSN presumably only has stations on the western side of the Gulf of Aqaba. It appears natural to assume that when common events are found in the catalogues, the readings are combined to construct just one event. However, the authors state that "priority was given to the data of the ENSN" (L124), which leaves me in a state of confusion what they have actually done. I think this should be clarified. And what time period are the data from? Maybe it would also be good to indicate (with e.g. a colour coding) which stations in Fig. 3 belong to which network.
REP: We have added more details to the description about the data merging to address this issue (L115–118). In addition, we have added a map showing separate symbols for the ENSN and ISC stations (Fig. 2).

2) The authors mention that data from "approximately 300 seismic stations" (L127) were used, but "only 53 of the stations were located in the study region (Fig. 3)". In Fig. 3, I am not able to understand what the study region is. Is the study region the entire area in Fig. 3? If so, why is a smaller area shown in Fig. 4 (and onwards)?
REP: In the updated Fig. 2, the left plot is a general map of the study region with all stations used in this study. The right plot limits are exactly the same as in the resulting figures.

3) On L125 the authors state that their data "are part of a dataset that covers a much larger area than presented in the resulting maps. This helped us avoid some of the edge effects that occurred when stations and/or events were located close to the limits of the processed area." I am confused. In what sense is it an advantage? Do they mean that they use station and events outside

the study area? How are then the parts of the rays that fall outside the study area accounted for? Fig. 4 appears to show raypaths coming from outside into the (study?) area – which to me suggests this is actually what they do. But how?

REP: We have added the following sentence clarifying this issue: "Using the stations and events from a much larger area surrounding the region of interest enabled us to improve the azimuthal coverage and increase the number of picks for some events" (L115–116).

4) No travel time vs offset plots are shown. I think this would be helpful, as it appears from the cross-sections in Figs. 8 and 9 that also the upper mantle is modelled. Then I assume that Pn- (and Sn-)phases are used. If so, are those phases also used to locate the events?

REP: We have added Fig. 3, which plots the travel times versus epicentral distances in the initial catalog, as requested by the reviewer. We have also added some descriptive text related to this figure (L126–127).

Modeling procedure:

5) How many unknown model parameters do the models contain? Table 1 tells that the model cells are 10x10x3 km in dimensions. Though no km-scale is given in any of the figures (and the model is possibly extending outside what is shown in the panels) I estimate that the models are at least 380x250 km horizontally and 69(?) km vertically. This results in nearly 44,000 unknown model cells (minimum) for the P- and S-models combined, plus 9000x4 unknown hypocentral parameters. This totals about 80,000 unknowns, which is about the same number of data – yielding a (slightly) over determined P-model and an underdetermined S-model. I find this information crucial, and suggest the authors account for it.

REP: We have added more details to the description of the grid construction (L144–150). Actually, the nodes were installed only in areas with sufficient amounts of data. In the vertical direction, the grid spacing was usually larger than 3 km depending on the ray coverage. Therefore, the number of nodes was considerably less than that estimated by the reviewer. On the other hand, the results would not be invalid if the number of nodes was larger than the number of data. Indeed, all the velocity parameters are linked with each other through smoothing equations, and they cannot be considered as independent. In our algorithms, we prefer to always use grid spacings much smaller than the resolution capacity to avoid grid dependency of the results. The resolution of the solution is merely controlled by the smoothing coefficients.

6) It appears that the crustal thickness varies significantly within the model (from 20 to 40 km, L228-230). Yet there is no velocity discontinuity in the model at the crustmantle interface (Table 2). The authors acknowledge (L311) that there is a trade off between crustal velocities and crustal thickness. Though it is tempting to read a crustal thickness from the cross-sections in Figs. 8 and 9, what is the iso-velocity they used to define the crust-mantle boundary? Maybe it would be nice to see some hypothesis tests on allowed variation of crustal thickness vs (lower) crustal velocities?

REP: Thanks for this comment; we have added a new test in Fig. 6 in which we explore the possibility of estimating the Moho depth variations based on the continuous tomography models. We have also added a paragraph describing this test (L206–219).

7) On the same theme: The authors first identified a 1D starting velocity model using "trial" (and error?) – L167). Considering the large variation in crustal thickness in the area, I assume that the event distribution would largely control what 1D model is "the best". One could also imagine a different procedure acknowledging the large variation in crustal thickness, and assigning a different starting model to the different model regions. Maybe the authors should explore this option – or at least provide argument against it.

REP: We provided more details on estimating the starting 1D velocity model (L160–170). We do not understand how different 1D models could be assigned to different regions? What would happen on the boundaries? How we can compute travel time if a ray path passes through different zones. We suspect that such artificial subdivision of the area would strongly affect the final result.

Structure of the paper:

In addition to splitting the "Introduction" into two separate parts (see above), it is a bit confusing to me why the "Data and Algorithm" is not in separate sections.

REP: In the new version of the paper, each of these two sections are separated into two separate parts.

In my view it would improve the paper if they were kept separate. Similarly to the "Results" section which contains information of both the synthetic reconstruction tests and on the results from the real data. I also suggest the authors go over once more what belong in the "Results" and what in "Discussion", it appears to me that there is some repetition.

REP: The sections with Results and Synthetic modeling information have been separated. The issues related to the discussion have been moved to the Discussion section from the original Results section.

Also, there are new things appearing in the "Conclusions" that have not appeared before, e.g. the comparison with the model of Eastern Mediterranean (L367). This is not a "conclusion" to me, but a "discussion".

REP: This statement has been moved to the Discussion section.

Other questions/comments:

Line 2: depths of what?

REP: We have added the phrase "with the bottom depth…" for clarity.

L31-34: unclear sentence – e.g. what do "this" and the double "it" refer to?

REP: We have rewritten these sentences as follows: "This sedimentation regime differs from the Gulf of Suez, which is located on the other side of the Sinai Peninsula. Many consider the Gulf of Suez to be a zone of ongoing crustal extension (McClusky et al., 2003; Mahmoud et al., 2005), and it is nearly fully covered by young sediments (Gaullier et al., 1988; Cochran and Martinez, 1988)" (L98–100).

L40: One of the largest faults in the world? Reference, maybe?

REP: This statement has been removed from the text.

L49-50 and L72-74: A variable displacement of the fault (Garfunkel, 1981) is not consistent with a model as shown in Fig. 2. Is this an outstanding geologic controversy? If so, I think the authors should bring it out more clearly that they want to try to address it. Or – considering the age of some of the references, is this controversy solved long ago? If so, is it at all relevant to account for it here?

REP: We present a rather simple model without considering the difference in slip rate in different parts of the DST. Otherwise, this would require more sophisticated modeling tools and it could not be accomplished within this tomography study. For the purpose of qualitative interpretations of our tomography results, such a "scissor and paper" model is sufficient to illustrate our hypothesis. We have made some changes to the description of this model (L321–327).

L140 and L146: The tomography algorithm they use account for the sphericity (curvature?) of the Earth, but uses an approximate raytracer (the "bending method"). To me it appears that for a model region this small the latter would generate much larger errors than using a "flat" Earth would. Or am I wrong? Maybe the authors could motivate their choice in this regard.

REP: We have added the following sentence: "This is especially important for rays with long offsets displaying regular bias if sphericity is not taken into account (in a flat model, travel times are always slower)" (L138–139).

L163: Many of the parameters in Table 1 is completely incomprehensible. For example, what does an "Amplitude damping, P and S" of "0 and 0" mean?

REP: Some parameters, which were not important, have been removed from this table.

L182: Are the synthetic travel times computed with the same (forward) algorithm as in the inversion? If so, 1) why iterate that it is a "bending method"?

REP: The ray paths in the synthetic model and those used for tomographic inversion are considerably different. The first reason for this involves the difference between the starting 1D model and "unknown" true 3D velocity model. Second, we start the analysis from the location of sources in the 1D model, which results in considerable shifts of some events. Iterations are necessary to bring back, as much as possible, these events toward their true locations and to build ray paths in the updated 3D models.

And 2) the authors are in fact committing the (very common) "inverse crime", i.e. doing the same approximation (error) in the forward as the inverse computations, thus the errors in some way cancel. As the "inverse crime" is so common, the authors may be forgiven, but maybe they should (as stated earlier) explore a little bit what limits in model perturbations (in amplitude and wavelength) are OK for the ray bending approximation.

REP: Actually, we have never heard about using more realistic forward modeling in such types of problems. If, for example, we perform elastic wave modeling and obtain full waveform seismograms, then picking these data will take an unrealistically long time. Certainly, it does not make sense to do this for our purposes.

L204-205: No, the resolution in the P- and S-models do not appear to me to be similar (see 1 on "Modelling procedure" above).

REP: We have removed the phrase regarding the statement on the similarity.

L235: That the P- and S-wave models are similar may also be an effect of Vp/Vs ratio damping – if such a constraint is applied. And it is not obvious to me as I do not understand all the algorithm parameters applied.

REP: No damping for the Vp/Vs ratio was applied! In this sense, the P- and S-anomalies are independent (only slightly linked through source parameters) (L153–154).

L309-310: No, it is not clear at all to me.

REP: This part of the discussion has been removed.

L317: "to similar to" – huh?

REP: This sentence has been rewritten.

Figures:

The figures are generally OK, but a km-scale would be helpful in most of them.

REP: We have created kilometer distance scales for all maps where there were no other kilometer scale indicators (i.e., such as locations of the profiles).

Anonymous Referee #2

General Comments:

The reviewed paper shows the results of the tomographic inversion of P- and S-wave travel times in the Gulf of Aqaba. I really think that the results presented in this manuscript are very interesting, providing new valuable information to understand the structure beneath the Gulf of Aqaba and the geodynamics implications derived from that. For this reason I think that this manuscript is clearly within the scope of SE. Nevertheless, the present manuscript needs of major revisions to be suitable of being published in this journal. First of all the manuscript has a problem of organization because is not following the standard structure of a scientific paper. The different sections do not contain what it should be expected.

REP: The text and organizational structure of the paper have been considerably reformatted (see other replies).

A clear example is the Introduction that it is a mixing of Introduction, general knowledge and geological setting.

REP: We agree with this comment and separated the Introduction text from the Geological setting text.

But sections such as the Results or the Discussion are also very confusing and they need a hard work to make them suitable for publication.

REP: The Results and Discussion sections have also been reformatted considerably in response to all the reviewers' comments.

Another issue to considerer (in some point it is related with the organization problems) is to clearly state which is the main purpose of the presented work. This is really important because this is the reason why the authors are written the paper. Obviously, if it is clear the paper is easier to organize. In any case, all these issues will be addressed in more detail in the Specific comments.

In spite of these general comments I really encourage to the authors to work in this manuscript because I think that the results contained on it are a significant contribution of the knowledge of the study area.

Abstract: this part of the manuscript needs to be rewritten. The abstract should include the purpose of the investigation (at the beginning), the methods used, the major findings and finally a brief summary of the interpretations and the conclusions. In my opinion, in this abstract the purpose of the work is not clear (only a description of the area is done), and the interpretation and conclusion (a brief summary) are missing.

REP: The abstract has rewritten according to these recommendations.

Introduction:

This part of the paper is really confusing and needs a hard work. An introduction should content three main parts: i) a general context of the problem that will be addressed in the paper including a summary of the existing knowledge and the current situation. ii) state the purpose of the work and iii) a brief explanation of your approach and what you can obtain from it to provide a solution to the problem. This is not accomplished at all in the Introduction of this manuscript.

REP: In the annotated version of the manuscript, we have indicated subtitles (red font) according to the plan proposed by the reviewer. These subtitles can be removed from the main manuscript before publication.

The first problem is that the Introduction includes a mixing of Geological Setting and Introduction that should be fixed. Move all the significant (important according to the problem presented in the manuscript) geology that helps to understand the study area to a new section. This will make a huge difference that it will help the reader to follow the manuscript.

REP: According to this recommendation, a new section titled "Geological setting" has been created.

After moving the geology to a new section the Introduction should have more fluency. The structure should move from general information and focusing down to the specific problem the authors studied. For example, the first paragraph of the Introduction (L23-L34) is an example of that. It is just a description of several features: seismicity, evidences of tectonic processes because of the bathymetry and sedimentation rates. How are they related to the problem described in the manuscript? What is it relevant for your study?

REP: We tried to reorganize the Introduction in response to this advice. We hope we understood the reviewer's comments correctly.

Another important thing observed in the Introduction is to clearly point out who is the author of the statements presented there. For example (between L70-L74), in the description of the Fig. 2 several statements are done: "left-lateral displacement and the rotation". Where is this information coming from? Garfunkel, 1981 or Eyal et al, 1981? Or is coming from other source?

REP: We have added here "According to our reconstruction…" (L329–331). So, we make the reconstruction to achieve the best fit of the main basins along the DST, and then compare it with estimates made by other authors.

This fact is also observed between L76-L81 talking about the pull-apart mechanism. Which is the source used? The bibliographic quotes should be located in the right place to support the statements done in the Introduction. (NOTE: remember that this a comment about the Introduction but probably this paragraph should be in Geological Setting if this is considered for the authors).

REP: We have indicated the appropriate references for the pull-apart mechanism (L103-104) and (L336).

The last paragraph in the Introduction is the first place where the authors clearly states why they are doing all this work. Basically it consists of filling the gap between the crustal and upper mantle studies. This should be clear from the beginning (Abstract and Introduction) and it is not.

REP: The Abstract and Introduction have been revised.

Geological Setting:

All the information regarding to the geological context, regional and local, should be moved to this new section.

REP: We did this in accordance to the reviewer's recommendation.

Data and Algorithm:

This section is pretty fine but several issues should be addressed:

L122-L124: The authors state that the events coming from different catalogues were merged into one catalogue list. Is this a direct merging or is there any data quality control? If I correctly understand the authors are using existing arrival times and they don't carry out new picking.

REP: We already used picked data from the catalogs.

So I don't know if the confidence of the travel times coming from different catalogues should be taken into account. I think that more information about that should be included. Are both catalogues using different stations? Why are the authors giving priority to ENSN for the same event?

REP: We mostly used events located within the ENSN network because they had better location parameters than those provided by the ISC.

Are the stations presented in Fig. 3 from ENSN, ISC or both? A few sentences explaining that should be necessary.

REP: We have added a few sentences specifying the procedure for merging the ENSN and ISC data (L115–118). In Fig. 2, we have added a plot with the regional data distribution and depicted the ENSN and ISC stations with different colors.

A figure including example of the data and the quality of the picks used in the inversion could be interesting. In the manuscript the authors describe that the low magnitude of the earthquakes used and the sparse seismic network used provided a limited number of picks for every event. This is a good reason to show examples of the data to demonstrate their quality.

REP: In this study, we absolutely did not touch any waveform data and only used the catalog data picked by others. Therefore, it is hard to present any example for picking. Unfortunately, we could not address this reviewer's comment.

L124-131: In this part of the section, the authors explain the data base used in this manuscript. It seems that the same data set used in the Gulf of Suez study is the one used in this work. They claim that only 53 (of almost 300 stations) are located in the area of interest but it seems that they used other stations outside the area during the inversion. This is clear in Fig. 4 where the ray paths are plotted. Taking into account that it will be great to see all the stations used in this study that maybe can help to understand why they were used. A figure including all the stations and the study area will be much better. (REP: The new Fig. 2 provides this information.) The other question is to understand what "marginal effects" really means. Do you need better azimuthal coverage for event location? Including stations out of the study area allow you to use seismic events with less than 6 picks? This part needs more information. (REP: We have added a sentence addressing these questions in L126–127.)

L137-139: To remove the outliers, the authors use absolute residuals of 1.5 and 2.0 seconds. Is it a standard criterion established/used elsewhere? If it is not, could you explain a little bit more why you are using these values?

REP: We have added a sentence addressing these questions in L120–121.

Table 1: This table is really confusing. Most of the parameters are not relevant and difficult to understand their meaning and how significant are those values for the inversion. Keep the relevant values.

REP: We have removed a few lines that described non-relevant parameters.

L165-174: The selection of the initial 1D P-wave velocity model and the Vp/Vs ratio is not clear. Several questions should be addressed in this part of the manuscript. The choice of an appropriate initial model is pretty important to obtain the right

relocation of the events and obviously the best final 3D velocity model. Reading the text is unclear which criterion is used to build the initial model and the Vp/Vs ratio. (REP: The main criteria used were the minimum number of rejected picks and minimum average residual deviation.) The authors state that they used a trial method to find the best initial method. How are they building these models? (REP: In each case, we changed the values of the Vp/Vs ratio and P-velocity at one or several depths and then performed the location analysis of events in this model. Furthermore, we made several trials of full iterative tomographic inversion to be sure that the best model provides a balanced amount of positive and negative anomalies at all depths.) Are they using previous information? (REP: No a priori information was used.) How many initial models are used? (REP: ~20; L163.) How do the authors modify the different models tested?

REP: We have changed the description for the optimization of the 1D model and addressed all the reviewer's questions (L160–170).

Furthermore, looking at the final velocity models and the variability of the crustal thickness it seems to me that the use of only 1D model for all the area can condition all the results. Is it possible to build more sophisticated initial models (2D for example) to account for lateral crustal thickness variation? Is it possible to estimate the robustness of the final model in relation to the chosen initial model?

REP: If we had a robust trustworthy crustal model for the entire region, it would make sense to use it as a 3D starting velocity model. In our case, not much information on the Moho depth is known. Any predefinition of the 3D velocity structure would affect the results. Thus, it would be not easy to distinguish whether the structures we observed were due to the predefined model, or whether these were really actual structures.

Table 2: Is this table necessary? Maybe a figure showing all the initial models used and the chosen one, including the parameters that reveal this model as the best one, will give more information about the initial model building.

REP: In our opinion, numerical values in tables are more relevant than graphs on a figure, as they can be directly used by other scientists in their calculations. Therefore, we prefer keeping this table in the paper. However, if the editor insists, we can easily construct the requested figure.

Results:

This section also needs a new organization. The checkerboard tests could be included in a separated section, something like Resolution tests. Two figures of the paper are dedicated to synthetic tests so probably a section should be necessary.

REP: According to this comment, we have created a separate subsection titled "Resolution tests".

Several comments about the checkerboard tests:

Which is the unperturbed velocity model used to create the synthetic travel times? Is the tomographic inversion using the same initial 1D model and Vp/Vs ratio? I guess so.

REP: We have added the following two sentences to address this question: "The synthetic anomalies have been added to the reference 1D velocity model with constant Vp/Vs ratios. In this specific case, this reference model is presumed to be known" (L185–186).

About the horizontal resolution test I have several comments. First of all, this is a results section so what we expect is a more detailed description of the obtained images. For the horizontal sections only one sentence (L195-197) is used to explain the checkerboard tests. You need a more description of what you see in the sections. Did you try other size cells? If 50x50 km is

the smaller one that it is offering a nice result? Which is the implication of that in the anomalies interpretation? What is happening at 50 km? I guess that at this depth you are not retrieving the data so this is the reason you are presenting only sections from 10 to 40 km.

REP: We have added a paragraph that considers all these issues (L187–193).

Use that to introduce the explanation of the results observed at different depths and remove the sentence "The reconstruction of this model is presented at four depths level". This should be a sentence for the figure caption.

REP: This sentence has been removed from the text and added to the figure caption.

The same comments can be applied for the vertical resolution tests. Most of the paragraph is used to explain how the checkerboard tests are created and plotted and only a few sentences to explain the results and their implications over the results.

REP: We have added several phrases describing the vertical resolution in different parts of the study area (L201–205).

Furthermore, in L202-205, the explanation of the vertical resolution tests is pretty unclear. The text: "The presented results were obtained from the reconstruction of. 4th sections were defined" is very confusing. This part should be rewritten to clearly understand what the authors exactly did.

REP. These sentences have been completely rewritten (L197–199).

Moving to the description of the travel time inversion, several issues need to be addressed: The description of the Results is very poor and probably some of the information in Discussion should be here. In this section you should describe objectively your key results in a logical sequence, without interpretation and supporting your comments with the figures. The Results section should show the evidences needed to answer the questions that you are trying to investigate in this work and they will be interpreted in the Discussion section. This is not done in this section.

REP: We have added a large block of the text containing a description of the main patterns that we observed in the resulting figures (L235–256).

The authors should introduce how they are presenting the results and why they are presenting in this way (anomaly maps, absolute values, the vertical sections, the colour scale used to make easy the correlation with geological features, etc.).

REP: We have added a comment regarding the development of the color scale for absolute velocities (L253–256).

In this description the information should appear in a coherent sequence and not just a sequence of sentences without any connection that are basically a description of a figure (should be in figure caption) or sentence ponting out what is plotted in a figure. An example of that is the text from L220-228. The figures are complements to understand what the authors are explaining in the text.

REP: We have considerably updated the text. The description of the results now follows a coherent progression from the shallower to deeper sections.

After that the authors should describe the results observed. They should prepare the reader for the interpretation and discussion. It is important to point out what is relevant in the results but from a objective point of view. This should be the Results section. This is not achieved in this manuscript. For example, in the paragraph between L220-224 the authors describe how they plot the figure (much of this information could be in the figure caption) and nothing is explained about the Fig. 7. What do we see in this figure? (REP: See the above comments.) Why are you not plotting this figure in absolute values? (REP: In figures with

absolute velocities, we also provide one horizontal section with absolute velocities; see Figs. 9 and 10.) You need to describe the main features that they will give you the support in the Discussion section.

In this section is very important to support the text with a figure quote. For example, if the authors are talking about one figure it should be easy for the reader to know which figure they are referring to. The question is make easy to the reader to follow the description of the Results.

REP: We have added more references to the figures within the text.

L236-240: The last paragraph is unnecessary. The authors should talk about the similarities and differences of two velocity models and what they mean related to the objectives proposed in this work. If the results are presented in a manuscript it means that objective parameters related to the inversion are assuring the quality of the final models (convergence, checkerboard tests, ...). They cannot use this argument (at least not in the paper) as a robustness test of the model.

REP: In our opinion, stating the correlation between the P- and S-anomalies is an important message that should be presented in the paper. Personally for us, if structures in P- and S-velocities are completely different, this looks very suspicious. In nature, at least on a regional scale, P- and S-anomalies usually behave similarly (e.g., the slab is always "blue" and the plume is "red"). If P- and S-structures are different, this should be a reason for special checking and discussion. The discussion on this issue is important to us. We have moved the relevant text up and removed the last sentence about verification (L232–234).

Discussion:

The Discussion is a complete mess. Obviously the lack of a good description of the Results makes really difficult to build a logical sequence in the interpretation and discussion of the results. The authors should use the Results section to show the main features observed in the velocity models, focusing in those that are relevant to address their objectives. (REP: In the new version of the paper, all relevant features has been described in the Results section.) When all the features are well described to the reader they should give an interpretation of all of them according to the objectives described in the Introduction. (REP: In the Introduction (L34–43), we have added information for several key questions that were considered based on our results in the Discussion section.) That means that every relevant feature observed need to be explained, if it's possible (if not it has also to be explained) providing a general picture of the study area to derive geological, geodynamic or tectonic implications.

Furthermore these implications need to be based in facts or at least an hypothesis that can be supported by other authors or similar works. For example, in L261-264 petrophysical hypothesis are proposed but any explanation for that is given. Any reference to seismic velocities expected for these petrologies (at this depths and geological context) or reference to other works in similar geodynamic context.

REP: We have added a reference to a review paper that describes typical values for seismic velocities in the felsic and mafic crust; that paper was authored by Rudnick and Fountain (1995).

The Discussion needs to be rewritten.

REP: We have considerably reformatted the Discussion section and added subheadings to improve the organizational structure.

In addition, the discussion of the results need to be clearly supported by the figures. In most of the Discussion the references to the figures are completely missing. There are plenty of reference to the horizontal sections, vertical sections, absolute velocity, 30 km section, but the figure number is not there. In this way, it is impossible to follow the Discussion and objectively appreciate the implications of the results presented in this paper to the knowledge of the study area.

REP: We have included references to the figures in many places within the Discussion.

Conclusion:

In my opinion, Conclusion section contains a lot of information that should be in Discussion. It is the only section in the manuscript that finally provide to the reader of a clear description of the objectives and how this work is trying to provide solutions to them. The authors should follow this to reorganize the paper.

Technical corrections:

L93: Author name is different in the reference list and the text. It should be Ginzburg if I'm not wrong. In this line is written Ginsburg.
REP: Corrected. Thank you.

L76: Add the reference to which plot: "In this plot" (Fig. 2) or use "In Fig. 2" instead of. The text must be clear to the reader.
REP: Corrected as recommended.

L112: In the Abstract and Data and Algorithm section two different sources for the data set used in the manuscript are meant: ENSN and ISC. In this line only the first one is used
REP: Corrected. Thank you.

L118: Change "from seismicity" and use, for example, "seismic events"
REP: This has been changed to "earthquakes".

L142-143: Add bibliographic references about other tomographic studies using LOTOS code
REP: We have added a reference to the web site where all the user manuals and source codes are stored. Just adding some other tomography studies not related to this story seemed inappropriate to us.

L150-151: Remove this sentence: "The distribution of the parametrization nodes, together ...". This is the description of the figure and it is located in the figure caption. Within the text, the reference to a figure is just to support the text. It is not necessary to include a sentence describing the figure.
REP: This sentence has been rewritten.

L161-162: Remove the sentence: "Values of the main parameters used..." for the same reason that the previous comment.
REP: In our opinion, this short sentence is necessary as it introduces Table 1. The sentence was therefore retained.

L215: Which is the value of the picking accuracy reported by ENSN? If you know the value it will be great to compare with the residuals reduction.
REP: We have added the estimates for the picking accuracy, i.e., 0.1–0.15 s for the P-phases and 0.15–0.2 s for the S-phases (L222–224).

L220-224: This paragraph should be rewritten and included in a more exhaustive description of how the velocity are plotted and why they are plotted in this way. The paragraph, in the way is written, seems more a figure caption than a Results description.

REP: The relevant text containing the description of the results has been completely rewritten.

L225-228: This should be written together with the description of how the velocity models are presented in this manuscript. If the authors are using this colour scale in order to make easy the correlation with geological features you should clearly explain that.

REP: A more detailed explanation on the development and use of this color scale has been added to the Results (L253–256) and Discussion (L282–285).

L243-244: Again, do not present what is in the figure. Talk about the horizontal sections and support that with the reference to Fig. 7. The same for the other figures.

REP: We tried to avoid repeating the information in the text and figure captions throughout the manuscript.

Figures:

Something observed in most of the maps is the lack of a scale (distance). I know that the maps are geographically referenced but it could help.

REP: We have created kilometer distance scales for all maps where there were no other kilometer scale indicators (i.e., such as locations of the profiles).

Figure 1. The authors refer to this figure talking about the depths reached for the Gulf Aqaba sea floor. If this information is relevant and they are using the colors to identify different depths in the figure, a color scale should be included.

REP: A color scale for the bathymetry is presented in Fig. 1.

Figure 3. I referred to this figure early in my comments. In my opinion all the stations used in the inversion should be included with a label (different icon used of color) for the different Institutions instruments. The study area should be indicated within this more general location map. A legend indicating this information will be also useful.

REP: We have added a large-scale map that includes stations from the ENSN catalog and those from the ISC catalog, and these different types of stations are represented with different colors (Fig. 2); a small-scale map related to the study area was also included.

Figure 6. The orientation of the profiles should be included in both corners of every section. We don't have a location map for them so we need to know how they are oriented.

REP: Actually, the km marks indicated in the map exactly correspond to the distance scale in the vertical section. This gives us an unambiguous reference.

Figure 8 and 9. The same for this figure. The orientation of the sections should be also in the sections.

Figure 10. Legend for the structural features presented in this figure.

REP: We have added a description for the red dotted lines (dykes). The other symbols were already explained.

Seismic structure beneath the Gulf of Aqaba and adjacent areas based on the tomographic inversion of regional earthquake data

Sami El Khrepy[1,2], Ivan Koulakov[3,4], Nassir Al-Arifi[1], and Alexey G. Petrunin[5,6,7]

[1]King Saud University, Riyadh, Saudi Arabia, P.O. Box 2455, Riyadh 11451, Saudi Arabia

[2]National Research Institute of Astronomy and Geophysics, Seismology Department, NRIAG, 11421 Helwan, Egypt

[3]Trofimuk Institute of Petroleum Geology and Geophysics SB RAS, Prospekt Koptyuga 630090, Novosibirsk, Russian Federation

[4]Novosibirsk State University, Novosibirsk, Russia

[5]Goethe-University, 60323 Frankfurt M, Germany

[6]GeoForschungsZentrum-Potsdam, Telegrafenberg, 14473 Potsdam, Germany

[7]Schmidt Institute of Physics of the Earth, B. Gruzinskaya 10, Moscow, Russia

Correspondence to: Sami El Khrepy (k_sami11@yahoo.com); Ivan Koulakov (ivan.science@gmail.com)

Contact information for other authors: Nassir Al-Arifi (nalarifi@ksu.edu.sa); Alexey G. Petrunin (Alexei@gfz-potsdam.de)

Submitted to *Solid Earth*
April 2016
Novosibirsk, Riyadh, Potsdam

Abstract. We present the first 3D model of seismic P- and S-velocities in the crust and uppermost mantle beneath the Gulf of Aqaba and surrounding areas based on the results of passive travel time tomography. The tomographic inversion was performed based on travel time data from ~9000 regional earthquakes provided by the Egyptian National Seismological Network (ENSN), and this was complemented with data from the International Seismological Center (ISC). The resulting P- and S-velocity patterns were generally consistent with each other at all depths. Beneath the northern part of the Red Sea, we observed a strong high-velocity anomaly with abrupt limits that coincide with the coastal lines. This finding is suggestive of the oceanic nature of the crust in the Red Sea, and it does not support the concept of gradual stretching of the continental crust. According to our results, in the middle and lower crust, the seismic anomalies beneath the Gulf of Aqaba seem to delineate a sinistral shift (~100 km) in the opposite flanks of the fault zone, which is consistent with other estimates of the left-lateral displacement in the southern part of the Dead Sea Transform fault. However, no displacement structures were visible in the uppermost lithospheric mantle.

Key words: Seismic tomography, Gulf of Aqaba, Dead Sea Transform, Northern Red Sea

1 Introduction

Tectonic activity in the Gulf of Aqaba region is responsible for high levels of seismicity, which represent a significant hazard for the local population. For example, in 1993 and 1995, two strong earthquake sequences with magnitudes reaching Mb = 5.8 and Mb = 6.7 (main shocks), respectively, occurred beneath the Aqaba basin (Abdel Fattah et al., 1997; Hofstetter, 2003). Understanding deep tectonic mechanisms is important for better assessing the seismic hazard in this region. However, there are still several important questions regarding the geodynamics of the Gulf Aqaba region and surrounding areas that have not been resolved, and these are the active focus of several debates among specialists in different domains of the geosciences. One of the issues relates to the nature of the opening of the Red Sea northern segment. Specifically, it is still unclear whether this feature results from stretching of the continental crust or from spreading and formation of the ocean-type crust. Several

other open questions relate to the mechanisms of origin and evolution of the Dead Sea Transform (DST) fault. In particular, it is still being debated which partition of the lithosphere (only the crust or the entire lithosphere) is involved in the strike-slip displacement along this fault zone. In addition, there are several alternative hypotheses related to the opening deep basins of Aqaba and the Dead Sea along the fault zone. Solving these and other geological problems requires robust information on the deep crustal and mantle structures.

There are distinct differences in the amount of studies that have previously examined different segments of the DST. The most comprehensive studies have been performed in the area of the Dead Sea (DESERT Group, 2004; Weber et al., 2009). Notably, several passive and active seismic experiments at different scales, receiver function investigations, and magneto-telluric studies have provided information on the crustal and upper mantle structures (Ritter et al., 2003; Mechie et al., 2005; Mohsen et al., 2006).

Unfortunately, most of these comprehensive studies only cover the areas around the Dead Sea and do not provide much information on the structures beneath the Gulf of Aqaba. Between the 1960s and 1980s, some reflection and refraction seismic studies used active sources to explore the detailed crustal structure beneath the Gulf of Aqaba, although primarily in the upper part (Ben-Avraham et al., 1979; Ginzburg et al., 1981; Ben-Avraham, 1985; Makovsky et al., 2008; Hartman et al., 2014). Seismic refraction data revealed a gradual southward decrease of the Moho depth from ~35 km at the northern edge of the Gulf of Aqaba to ~27 km in the southern part. These results helped identify some of the fault structures that can be used to explain the mechanisms of the opening of the Aqaba basin (Fig. 1b).

Several regional studies were performed for large areas of Asia and Africa that included the region investigated here. Large-scale surface-wave tomography studies by Park et al. (2008) and Chang and van der Lee (2011) did not reveal any particular features related to the Aqaba basin. According to the models of the crustal structure and Moho depth for the entire eastern Mediterranean region by Koulakov and Sobolev (2006) and Mechie et al. (2013), the crust to the north of the Gulf of Aqaba is locally thicker than that of other areas. A recently derived seismic model for the upper mantle beneath the Arabian region (Koulakov et al., 2016) gives fair resolution for the Sinai, Aqaba, and Dead Sea regions; however, it does not provide any information for structures above a 100 km depth.

This overview shows that between detailed seismic surveys of shallow structures in the Aqaba region and large-scale regional tomographic models, there is a gap related to studies of the crust and uppermost mantle beneath the Gulf of Aqaba and surrounding areas. Although there is active seismicity in this region and a fair amount of seismic stations on both sides of the Gulf of Aqaba, to date, no detailed earthquake tomography work has been performed here.

The purpose of this study is to close this gap and to present a new tomographic model based on a large dataset, which was provided by the Egyptian National Seismological Network (ENSN) and supplemented with data from the International Seismological Centre (ISC). The 3D models of P- and S-velocities allow another look at the structures beneath the Gulf of Aqaba and surrounding regions and enhance our knowledge of the deep mechanisms driving the geodynamic processes in this region.

2 Geological setting

The Gulf of Aqaba, which is also referred to as the Gulf of Eilat, is a basin located at the northern tip of the Red Sea, east of the Sinai Peninsula and west of the Arabian Plate. With the Gulf of Suez to the west, it extends from the northern portion of the Red Sea. The length of the Gulf of Aqaba is 160 km, and its largest width is 24 km. The maximum floor depth in the gulf reaches 1850 m. Politically, it is surrounded by four countries, viz. Egypt, Israel, Jordan, and Saudi Arabia.

The Gulf of Aqaba represents a transition zone from the spreading zone in the Red Sea to the DST characterized by strike-slip displacement (Ben-Avraham et al., 1979). A very similar transition occurs in the Gulf of California at the southern edge of the San Andreas Fault. Many researchers (Joffe and Garfunkel, 1987; Ehrhardt et al., 2005) accept that the opening of the

Gulf of Aqaba occurred simultaneously with the initiation of the DST 20–15 Ma ago. The DST can be traced for more than 1000 km from the Red Sea to the westernmost end of the Zagros collision zone in eastern Turkey; it cuts the continental crust along the eastern margin of the Mediterranean Sea. Global positioning system (GPS) observations provide rates of the present left-lateral displacement along the DST fault in the range of 3.5–4.0 mm per year (Wdowinski et al., 2004; Gomez et al., 2007), but geological data provide evidence for faster rates ranging from 5 to 10 mm per year of long-term displacements in the past starting from the initiation of the DST 20–15 Ma ago (Garfunkel, 1981; Chu and Gordon, 1998). On the basis of geological information, the total displacement in a segment of the DST between the Gulf of Aqaba and the Dead Sea has been estimated to be 105 km (Freund et al., 1968; Bartov et al., 1980; Garfunkel et al., 1981). To the north of the Dead Sea, the displacement is considerably less (Garfunkel, 1981).

The initiation of the DST was due to the relative displacements of the African and Arabian plates (Fig. 1a). In the no-net-rotation reference frame, the African and Arabian Plates both move northward, but their displacement vectors differ slightly in terms of their magnitudes and orientations (Smith et al., 1994; McClusky et al., 2003). This leads to the divergence of the African and Arabian Plates in the area of the Red Sea and results in spreading of this ocean-type basin. In the area of the Dead Sea and to the north, the displacement vectors of these plates are nearly parallel; however, the Arabian Plate moves faster, thus resulting in conditions for transform faulting.

Sharp bathymetry features of the Gulf Aqaba floor and the presence of deep-sea segments reaching depths of 1850 m (Fig. 1b) provide evidence for ongoing active tectonic processes (Ben-Avraham et al., 1979; Ehrhardt et al., 2005; Makovsky et al., 2008). It appears that in some parts of the Gulf of Aqaba, the sedimentation rate cannot compensate for the rapid subsidence of the sea floor (Ten Brink et al., 1993). This sedimentation regime differs from the Gulf of Suez, which is located on the other side of the Sinai Peninsula. Many consider the Gulf of Suez to be a zone of ongoing crustal extension (McClusky et al., 2003; Mahmoud et al., 2005), and it is nearly fully covered by young sediments (Cochran and Martinez, 1988; Gaullier et al., 1988).

Although the link between the opening of the Aqaba basin and the initiation of the DST displacement is generally accepted, details of this process are still debated. Most scholars associate the origin of deep linear depressions along the DST, such as the Gulf of Aqaba and the Dead Sea, with the pull-apart mechanism (Mann et al., 1983; Makovsky et al., 2008; Petrunin and Sobolev, 2008; Hartman et al., 2014). In this context, lateral displacements along a non-straight fault line should lead to the origin of compression and extension zones at the vicinity of the fault, and many studies have used both numerical modeling (Petrunin and Sobolev, 2008; Petrunin et al., 2012) and geological evidence (Ehrhardt et al., 2005) to demonstrate the possibility of such a scenario. Alternatively, the origin of the present depressions along the DST can be explained by the relative transform-normal extension (Ben-Avraham and Zoback, 1992; Smit et al., 2010) due to relocation of the pole of rotation for the DST at about 5 Ma (Garfunkel, 1981). Geophysical investigations of the crustal and mantle structures are one of the key elements required for deciphering the puzzle of the tectonic history of this region.

3 Seismic data

In this study, we used the arrival times of P- and S-seismic waves from earthquakes occurring beneath the Gulf of Aqaba and surrounding regions for the analyses. The dataset was mostly extracted from the catalogs of the ENSN, and it was complemented by data from the ISC catalogs to enlarge the study area and improve data sampling. The distributions of the stations corresponding to both databases are depicted in Fig. 2 with different colors. For each event recorded by the ENSN network, we searched for a corresponding event in the ISC catalog, and if we found such an event, the duplicate information was not recorded in the dataset. Additionally, if the ISC catalog had station data not presented in the ENSN, we added this information to our dataset. The quality control for the combined data was performed at the stage of source location. To remove outliers from the data, we selected the picks with absolute residuals of less than 1.5 and 2 s for the P- and S-data, respectively, which corresponded to the stage of source location in the starting 1D velocity model. These threshold values correspond to the estimated values of residuals along the existing P- and S-wave data caused by expected heterogeneities in the study area.

The data used in this study are part of a dataset that covers a much larger area than the region presented in the resulting maps (left panel in Fig. 2). The same dataset was used in a recent study by Khrepy et al. (2016), who provided information on the crustal and uppermost seismic structures beneath the Gulf of Suez. The data for this study were recorded by approximately 300 seismic stations in Egypt and surrounding countries; of these stations, only 53 were located in the study region (right panel in Fig. 2). Using the stations and events from a much larger area surrounding the region of interest enabled us to improve the azimuthal coverage and increase the number of picks for some events.

In total, we used more than 9000 events from an area covering all of Egypt (left panel in Fig. 2), of which approximately 3000 events corresponded to the Aqaba region and northern Red Sea (right panel in Fig. 2). To select the data for tomography analyses, we used a criterion of a minimum of 6 picks for any phase (P or S) per event. In total, we selected ~65,000 P-picks and ~17,000 S-picks, with an average of 9 picks per event. The relatively small ratio was due to the sparse distribution of stations and mostly low magnitudes of events. Figure 3 shows the travel times of P- and S-waves versus distance. For most of the ray paths (85 %), the epicentral distances were less than 300 km; however, data with distances of up to 700 km did exist, and these data provided us with information about the upper mantle.

4 Algorithm for tomographic inversion

The tomographic inversion was performed by using LOTOS (Local Tomography Software) code (Koulakov, 2009) expanded for the case of large areas. This algorithm accounts for the curvature of the Earth when computing the travel times of seismic rays. This is especially important for rays with long offsets displaying regular bias if sphericity is not taken into account (in a flat model, travel times are always slower). The details of this code have been described in the literature (Koulakov, 2009) and on a web site available at http://www.ivan-art.com/science/LOTOS. Here, we only briefly present the major steps and features. The workflow begins with a preliminary calculation of source locations based on the grid search method. For faster calculations, we approximated the model travel times by using a set of tabulated values derived at a preliminary stage. Then, the locations of sources were recomputed by using the 3D ray-tracing algorithm based on the "bending method" (Um and Thurber, 1987). The 3D velocity distribution was parameterized with nodes that were distributed in the study area according to the density of rays. The nodes were installed only in areas with sufficient data coverage (with ray densities larger than 0.1 of the average value). In the vertical direction, the distance between nodes was inversely dependent on the ray density, but it could not be less than 3 km. In horizontal directions, the grid spacing was defined as 10 km. The numbers of parameters for the P- and S-models were ~18,600 and ~10,600, respectively. An example of the parameterization node distribution, together with the ray paths, is presented in Fig. 4. To reduce grid dependency, we performed the inversions for four differently oriented grids with basic orientations of 0°, 22°, 45°, and 67° and then averaged the results. The inversion was performed simultaneously for 3D P- and S-anomalies, source corrections (four parameters for each source), and station corrections. The velocity solution was damped by a smoothing matrix, which minimized the velocity gradients between all neighboring parameterization nodes. No damping for the Vp/Vs ratio was implemented. In this sense, the P- and S-anomalies were inverted almost independently (they were only slightly linked through the source parameters). The inversion was performed by using the LSQR algorithm (Page and Saunders, 1982; Nolet, 1987). The steps involving source locations in the derived 3D models, the calculation of the first derivative matrix, and the inversion were iterated five times (a compromise between the computing time and accuracy of the solution). The values of free parameters (e.g., weights for smoothing, station and source corrections) were determined based on the results of synthetic modeling. Values of the main parameters used for the calculation of the main model are given in Table 1.

The data analysis began with finding an optimal starting velocity model. We used a fairly simple approximation that employed a 1D distribution of P-velocity and a constant value of the Vp/Vs ratio. The P-velocity was defined in several depth levels; between these depths, the velocity was linearly interpolated. The optimal model was determined by using the trial and error method. The initial location of sources (i.e., grid search with tabulated travel times) was performed in approximately 20

different models by using different P-velocities and Vp/Vs ratios. In each case, we changed the values of the Vp/Vs ratio and P-velocity at one or several depths and then performed the location of events in the model. The best model was the one that provided the minimum number of rejected outliers and minimum values of average residual deviations. Furthermore, we made several trials of full iterative tomographic inversion to be sure that the best model provided a balanced amount of positive and negative anomalies at all depths. Note that we performed the optimization for the entire dataset of the Egyptian networks; so, the resulting heterogeneities within the selected area of interest may appear not perfectly balanced. As a result of these procedures, we obtained an optimal Vp/Vs value of 1.74 and the P-velocity distribution presented in Table 2.

5 Results

5.1 Resolution tests

Before discussing the main velocity models, we present the results of synthetic tests used to assess the horizontal and vertical resolution. Synthetic data were computed by using the same ray configuration as that in the observed data catalog used to calculate the main tomography model. The synthetic travel times were calculated by using the algorithm for 3D ray-tracing based on the bending method. Random noise with a magnitude of 0.15 s was added to the synthetic travel times. Before starting the reconstruction, we perturbed the locations of events and origin times so their true values remained unknown. The reconstruction procedure included all of the steps performed during the LOTOS code procedure, including the preliminary location identification of sources in the starting 1D model. This step strongly biases the synthetic residuals and leads to a trade-off between the source and velocity parameters, similar to the processing of observed data. These synthetic tests helped us to derive the most optimal values for the inversion parameters, thus enabling the highest quality of reconstruction. The parameters were then used to perform the inversion of the observed data.

Here, we present results for three synthetic models. The first model (Fig. 5) was used to assess the horizontal resolution. In this case, cells with positive and negative anomalies with an amplitude of ± 5 % and a size of 50 km × 50 km were defined without depth changes. The synthetic anomalies were added to the reference 1D velocity model with the constant Vp/Vs ratio. In this specific case, the reference model is presumed to be known. The results in Fig. 5 show that this model generally recovered the anomalies well in most parts of the study area. The best resolution was achieved beneath Sinai and the Gulf of Aqaba, where we were able to restore both the shape and amplitudes of the anomalies. We also tried other checkerboard anomalies and found that patterns with smaller sizes of 25–30 km were still detectable in these areas. It is interesting that beneath the northern margin of the Red Sea, where we do not have stations, the synthetic structures can still be resolved correctly. At deeper sections (40 km), we observed some loss of resolution throughout the study area. However, while performing other tests with larger anomalies, we found that a fair resolution at 40 and 50 km depth could be achieved for pattern sizes starting from 80–90 km.

The second model (Fig. 6) was aimed at estimating the vertical resolution. Because of the trade-off between the source and velocity parameters, in most cases of earthquake tomography analysis, the vertical resolution is much poorer than the horizontal resolution. In this test, we defined checkerboard anomalies along the same vertical sections that were used for presenting the main results. Across the section, the thickness of anomalies was 40 km. To avoid overlapping synthetic anomalies in the case of intersections of different sections, we performed separate calculations for four models in which the synthetic anomalies were defined along a single profile. Here, we show the results for the P-model. We see that in most sections, the change in the anomaly sign at 15 km depth was correctly recovered. The anomalies between 15 and 45 km were only recovered in the presence of deep earthquakes, and in many cases, they were strongly smeared. Fair recovery of anomalies in this layer was achieved beneath Sinai (left parts of sections 3 and 4), where the anomalies appeared to be even clearer than the shallow anomalies above 15 km depth. The best resolution was achieved beneath the northernmost margin of the Red Sea

and southern part of the Gulf of Aqaba, where we were able to resolve the second boundary of change in the anomaly sign at 45 km. This test shows that the vertical resolution is strongly variable; this should be considered when interpreting the results.

The last test was aimed at checking the possibility of restoring the variations of first-order interfaces such as the Moho boundary. Normally, seismic tomography provides continuous velocity distributions, and it cannot be directly used for studying the geometry of interfaces with sharp velocity contrasts. At the same time, velocity variations in the corresponding depth interval may give information about the relative deviations of the interface depth. In the upper plot of Fig. 7, we present a synthetic model representing the crust with variable thickness. In this model, an anomaly of -20 % defined within a 3D polygonal prism representing the crust is superimposed with the reference 1D velocity distribution. After computing the synthetic travel times, we performed the reconstruction procedure with another 1D model. The recovered P- and S-velocity models are shown in the middle and lower plots of Fig. 6. Here, it can be seen that for the P-velocity model, the Moho interface can be associated with the iso-velocity line at 6.6 km s^{-1} (blue layer). The total variation of the Moho depth of ~20 km was reconstructed correctly, although the transition zone between "thin" and "thick" crust appeared smoother than that in the synthetic model. For the S-model, we detected a general trend of thickening and thinning of the crust, though the absolute variations of the velocity contour lines appeared smaller than the deviations of the Moho in the synthetic model. This test shows that the relative deviations of the main first-order interfaces can be investigated based on consideration of absolute velocities in vertical sections.

5.2 Inversion results

For the inversion of observed data, five iterations were performed. During the inversions, the average absolute residuals were reduced from 0.232 to 0.173 s (25.5 %) for the P-data and from 0.348 to 0.208 s (40.2 %) for the S-data. The values of the final residuals were generally compatible with the picking accuracy estimates reported by the ENSN (0.1–0.15 s for the P-phases and 0.15–0.2 for the S-phases). The larger reduction for the S-data seems to be paradoxical considering the lower quality of the S-picks. However, the S-data were more sensitive to velocity anomalies because the same percent value of an anomaly yielded a larger S-residual compared with the P-residual. In addition, the amplitudes of the S-anomalies were usually stronger than those of the P-anomalies.

The inversion results for the P- and S-anomalies are presented in horizontal sections in Fig. 8. For reference, in the section at the 10 km depth, we show the locations of the main faults. At the 20 and 30 km depths, we provide reconstruction markers for the left-lateral displacement of the DST, which will be considered in the Discussion (Sect. 5). Velocity anomalies are shown only in areas with a sufficient amount of data. Outside the resolved areas, the anomalies are shaded.

An informal argument for the robustness of the computed tomography models is the clear correlation of the main P- and S-velocity anomalies that were independent in inversion. Although P- and S-velocities should not necessarily fit each other, in practice, the main geological structures behave similarly in both cases, especially on a large scale.

The most striking feature, which was visible for both P- and S-anomalies at all depths in Fig. 8, was the prominent high-velocity anomaly beneath the Red Sea. The limits of this anomaly matched with the coastal line (especially at 30 km depth). The amplitude of this positive anomaly reached 10 %. As we can see in the checkerboard tests, the existing data configuration allows for robust recovery of this structure.

At 10 km depth (left column in Fig. 8), the areas to the north of the Red Sea look patchy, which is possibly indicative of the complex structure of the upper crust in this region. The similarity of the P- and S-anomalies and best resolution achieved at this depth in the checkerboard tests indicate the robustness of these structures. At 10 km depth, we did not observe any clear structures associated with the Gulf of Aqaba. We can only state that some alternation of anomalies in the opposite flanks of the gulf was detected. The Gulf of Suez at this depth is associated with a low-velocity anomaly.

At 20 km and deeper, the structures become more regular and less patchy. The Sinai Peninsula at 20 and 30 km depth (2nd and 3rd columns in Fig. 8) is mostly associated with a prominent low-velocity anomaly, whereas at 10 km depth, we

observed complex alternations of positive and negative anomalies. Beneath the coastal areas of the Arabian Plate and along the DST, we observed a large low-velocity anomaly. Together with the Sinai's anomaly, it forms a "zig-zag" shaped structure at 20 and 30 km depth following the coastal line of Sinai and Arabia.

At 40 km depth (right column in Fig. 6), the structure becomes rather simple. In the P-velocity model, we observed a straight diagonally oriented transition dividing the whole area in two parts, namely, a positive anomaly to the southwest and a negative anomaly to the northeast. In the S-velocity model, we still observed a remnant of the Sinai-related negative anomaly, which can be explained by the relatively poor vertical resolution of the S-model and downward smearing of crustal anomalies.

Absolute P- and S-velocities are shown at a 30 km depth with four vertical sections (Figs. 9 and 10). We have applied a special color scale to help highlight the main strata such as sediments (brown), upper crust (green and light blue), lower crust (dark blue), and uppermost mantle (red and yellow). Thus, the contour lines in the vertical sections roughly may represent deviations in the main interfaces.

6 Discussion

6.1 Comparison with previous studies

Previously, tomography results at the crustal and uppermost mantle scales for this region were lacking. While there have been several local scale offshore experiments in the northern Red Sea and in the Gulf of Aqaba (Ben-Avraham et al., 1979; Ginzburg et al., 1981; Ben-Avraham, 1985; Makovsky et al., 2008; Hartman et al., 2014), these studies mostly investigated the shallow structures beneath the sea floor that do not intersect with the resolved area of our study. The distributions of velocity anomalies shown in Fig. 8 can be compared with previous results on larger scales based on different methods. For example, in the regional tomography model by Chang and van der Lee (2011), the study area is entirely located within one large low-velocity pattern. The other regional tomography models mentioned in the introduction are also too rough to identify the details observed in the present model. Some similarities can be observed with the seismic velocity anomalies for the Aqaba region in the model by Koulakov and Sobolev (2006), which was based on data from the ISC catalogs, especially for the distributions of the S-anomalies. However, that area was on the margin of the model and thus had lower data density and poorer resolution. For the upper mantle, the P-velocity model is similar to a recent tomography model of the entire Arabian region by Koulakov et al. (2016), in which the southern part of the Gulf of Aqaba corresponds to the higher-velocity anomaly at 100 and 200 km depths. Meanwhile, the large area corresponding to the Dead Sea and surrounding region coincides with the lower-velocity anomaly.

6.2 Moho depth variations from tomography?

Normally, seismic tomography cannot be used for determining the depth of the first-order interfaces such as Moho. Specifically, tomography inversion provides the continuous distributions of anomalies for P- and S-wave velocities and it cannot restore sharp velocity changes. At the same time, some authors claim that in cases of varied interfaces with sufficiently strong velocity contrasts, velocity heterogeneities at corresponding depths may give information about the relative depth variations of the interface. For example, Koulakov et al. (2015), based on tomography work, have produced a map of the Moho depth variations beneath the central Himalayas. In that study, they used synthetic tests to show the resolving capacity and limitations of such an approach. In Fig. 7, we present a similar test showing that recovery of the Moho depth variations is possible in our case.

We propose that the absolute velocities can be used for estimating the Moho depth in the Aqaba region and surrounding areas. In Figs. 9 and 10 with the absolute velocities in vertical sections, we developed a special color scale that facilitates the tracing of certain velocity values possibly representing geological strata. For example, the brown color may represent sediments, green and light blue might be associated with the upper crust, dark blue possibly depicts the lower crust, and yellow and red are representative of the mantle. The contour lines of Vp = 7.3 km s^{-1} and Vs = 4.3 km s^{-1} (violet layer) are the average

values between the lower crust and uppermost mantle and may indicate the deviation of the Moho interface. On the basis of this assumption, we can estimate that beneath the Red Sea, the crustal thickness is approximately 20 km. The largest thickness observed was in the area of the DST (northern part of section 1) and beneath Saudi Arabia (northeastern part of section 2), where the Moho depth reaches ~40 km. A relatively thin crust (25–30 km) was observed beneath the middle part of Sinai (northwestern part of section 3 and southwestern part of section 4). The maps of absolute velocities at 30 km may indicate mantle velocities beneath the Red Sea (yellow and red) and crustal velocities in most of the surrounding areas (violet and blue).

Note, however, that these values should be considered as qualitative estimates of the Moho depth variations because of many additional factors that might also affect seismic velocities (such as velocity variations in the crust and mantle).

6.3 Oceanic crust in the Red Sea?

The main feature, which is clearly observable in both P- and S-velocity models at all depths, is the strong high-velocity anomaly that corresponds to the Red Sea. At the 30 km depth, the high velocity in the Red Sea may be related to a significantly thinner crust. In offshore areas, this depth corresponds to the mantle, whereas in continental areas, this is still the lower crust. The same conclusion follows from consideration of the absolute velocities along sections 1, 2, and 3 in Figs. 9 and 10. The high-velocity anomalies in the upper sections may support the notion that there is a prevalence of mafic rocks with higher velocities compared with felsic rocks, which is typical for the upper continental crust in surrounding areas (e.g., Rudnick and Fountain, 1995). This fact may renew debates regarding the nature of the crust in the northern Red Sea. According a concept proposed by some authors (e.g., Cochran and Martinez, 1988) that is based on the absence of clear signatures of spreading ridges and linear magnetic anomalies (e.g., McKenzie et al., 1970), the crust in the northern part of the Red Sea was formed as a result of gradual stretching, and thus, it has both felsic and mafic components. However, more recent studies (Cochran, 2005; Cochran and Karner, 2007) report clear axial depression of the bathymetry and aligned magnetic anomalies as well as a chain of dykes that are more typical for rifting processes. In our study, we can see that the high-velocity anomaly in the Red Sea has very sharp bounds coinciding with the coastline; this presumes an abrupt difference in crustal properties between the onshore and offshore areas at all depth intervals. This would mean that the upper felsic crust is almost absent at this area, and this would be not possible in the case of gradual stretching of the continental crust. We propose that such slow spreading might originate from a dispersed system of dykes covering large areas of the sea bottom. However, to prove this hypothesis, additional studies in other disciplines are needed.

At the 40 km depth, the structure corresponds with the uppermost mantle. As observed in synthetic tests, the vertical resolution of the S-model at this depth is poor. Therefore, it might be affected by the vertical smearing of crustal structures and the corresponding results do not accurately represent the distribution in the mantle. At the same time, the mantle structure for the P-velocity appears to be robust. The presence of high velocities in the uppermost mantle beneath the northern Red Sea at this depth does not confirm the hypothesis of significant hot asthenosphere upwelling, which would exist in the case of active rifting. This result supports the passive nature of the extension, which is likely due to relative displacements of large lithospheric plates, namely, the African and Arabian Plates. This looks consistent with the results of regional tomography work by Koulakov et al. (2016) in which the Red Sea is associated with high-velocity anomalies in the upper mantle.

6.4 Initiation and development of the DST

Our seismic tomography model provides new information on the crustal and uppermost mantle structures that may help to elucidate the details of the initiation of the DST fault and opening of the Gulf of Aqaba. In Fig. 11, we present the reconstruction of the displacements along the DST merely based on the analysis of the topography features that provide the most consistent fit of the basin limits. In this simple “scissor and paper” model, we do not consider the difference in slip rate along the DST, which seems to be not significant between the Dead Sea and Gulf of Aqaba (Garfunkel, 1981). We can see that the present locations of depressions along the DST can be explained by the relative transform-normal extension (Ben-Avraham and

Zoback, 1992; Smit et al., 2010) caused by the relocation of the pole of rotation for the DST at about 5 Ma (Garfunkel, 1981). The left plot in Fig. 9 depicts a possible structure before the initiation of the DST. In this reconstruction, the coastal structures form continuous trends in the NW–SE directions, which are indicated with red lines. According to our reconstruction, the present configuration, shown in the right plot in Fig. 11, was obtained by a left-lateral displacement of the Arabian Plate to ~100 km with a simultaneous counter-clockwise rotation to 2.7°. The total displacement is generally consistent with estimates made by other researchers, based on the similarity of geological strata (Freund et al., 1968). In this plot, red lines along the DST mark the location of the initial fault in the opposite flanks. Between these lines, there are extension zones that correspond to the Gulf of Aqaba and the Dead Sea. This reconstruction demonstrates the origin of the Aqaba basin resulting from simultaneous relative rotation of the Arabian Plate and an offset along the DST. For the Dead Sea, we have defined a step-shaped feature on the fault that facilitates the extension due to the pull-apart mechanism (e.g., Petrunin and Sobolev, 2008).

Here arises a natural question: can we detect the traces of this displacement in the crustal and uppermost mantle structures based on our tomography results? In Fig. 12, we present the back-reconstruction of the P-velocity seismic structures in the upper and lower crust corresponding to the lateral displacement modeled in Fig. 11. In the shallow crust (left column in Fig. 8), except for the large high-velocity anomaly beneath the Red Sea, the structures of the P- and S-anomalies are unexpectedly inconsistent with the distribution of the main geologic units. Neither the location of the Gulf of Aqaba nor the distributions of the main faults indicated on the maps at 10 km depth can be unambiguously associated with seismic anomalies. The seismic patterns in the Aqaba area look patchy and non-structured. However, as shown in the left panel of Fig. 12, after shifting the eastern flank with respect to the western one according to our back-reconstruction model, the structures become more consistent. For example, the negative seismic anomalies at the 10 km depth seem to form two continuously curved zones, which are highlighted with violet lines that appear to be nearly parallel. These anomalies may represent hidden geological structures that existed in the crust prior to the initiation of the DST fault. The complex shapes of these structures may have been due to intensive tectonic processes in previous stages of geologic development of the region. Note also that after back-displacement along the DST fault, the dykes identified by Fyal et al. (1981) (red dotted lines in the left plot of Fig. 12) seem to form consistent structures aligned parallel to the coast.

In sections at depths of 20 and 30 km in Fig. 6, we depict the markers of the lateral displacements since the initiation of the Dead Sea Fault with green dotted lines. The line along the coast, which has a step-shaped form after ~100 km of left-lateral displacement, almost perfectly fits the transition between high- and low-velocity anomalies. In the right panel in Fig. 12, we present the seismic structure corresponding to the stage just before initiation of the DST. Here, it can be seen that the transition between high- and low-velocity patterns looks almost straight. These reconstructions correspond well to the total estimates of the lateral displacements along the DST derived from independent sources.

6.5 Traces of the Aqaba and DST in the crust and mantle

The lack of a prominent anomaly beneath Aqaba (left column in Fig. 8), which was expected at shallow depths because of the sediments, may indicate a relatively thin sedimentary cover that does not considerably contribute to the seismic model. The Gulf of Aqaba has generally deep bathymetry, which indicates that the rate of extension here exceeds the sedimentation rate. According to seismic surveys by Ben-Avraham et al. (1979), the maximum thickness of sediments in the Aqaba basin may reach 2–3 km, but the thickness appears to be strongly variable. The sedimentation in the Aqaba basin appears similar to the average sedimentary cover thickness in the surrounding onshore areas and thus does not produce a prominent relative negative anomaly in the shallow velocities. Furthermore, the ray configuration used in this study does not allow for the recovery of shallow anomalies in the offshore areas. This can be compared with tomography results for the shallow water basin of the Gulf of Suez (left column in Fig. 8), which is completely covered with sediments and is where we observed a shallow low-velocity anomaly both in the P- and S-velocity models.

At deeper sections (2nd and 3rd columns in Fig. 8), we observed a negative anomaly along the northern segment of the Gulf of Aqaba and the DST, which is especially clear for the S-velocity model at 30 km depth in Fig. 8. This structure possibly indicates crustal thickening and local heating due to the slip-parallel extension of the basin. However, seismic anomalies only indirectly represent crustal thickness variations, and they are sensitive to only large deviations of the Moho depth. Other methods such as seismic reflection surveys or receiver function analysis would be more suitable for this purpose.

We can see that at the 40 km depth (right column in Fig. 8), which corresponds to the uppermost mantle, the structure of P-velocity anomalies is different from those in the lower crust and transition zone. This difference is less prominent for the S-velocity, probably because of the poorer vertical resolution that smears down the crustal anomalies to the mantle. In the P-velocity model, instead of the step-shaped contact zone identified at the 30 km depth, we observed a nearly linear transition oriented SSE–NNW between high-velocities to the southwest and lower anomalies to the northeast. The shape of this boundary looks very similar to that in the lower-crustal model after back-reconstruction as shown in the right panel Fig. 12. Thus, these findings seem to indicate that the uppermost mantle conserves its structure regardless of slip displacements along the DST.

There are other lines of evidence that the DST does not affect the mantle structures significantly. For example, the regional tomography model of the eastern Mediterranean by Koulakov and Sobolev (2006) shows a zone of relatively low P-wave velocity to the north of Aqaba continuously crossing the fault. Teleseismic tomography for the Dead Sea area (Koulakov et al., 2006) also did not reveal any fault related structures in the upper mantle. It is important that the existing models of the Moho depth in this region (see review in Mechie et al., 2013) do not reveal any clear connection with the displacement along the DST. However, it is not entirely clear how these continuous features in the uppermost mantle could be conserved after more than 100 km of displacement along the DST fault. All these examples suggest that most of the displacements along the DST occur in the crust, whereas the component of the strike-slip displacement rapidly decays with depth in the mantle lithosphere. Considering the relatively thin lithosphere (60–70 km), which has a tendency for southward thinning (Mohsen et al., 2006) in this region, one might assume that the anomalies in the mantle are mostly controlled by present-day thermo-mechanical processes in the lower-most lithospheric mantle and asthenosphere, rather than the displacements along the DST. However, this question still requires further investigations.

It would be interesting to study the relative velocity anomalies beneath Aqaba at depths that fully correspond to the mantle to identify the link between mantle processes and crustal displacements. Unfortunately, our model does not have sufficient resolution for depths greater than 40 km. At our scale and in our area of interest, information on mantle structures can only be derived from the analysis of teleseismic data. Our future work will focus on analyses of the teleseismic records provided by stations distributed over the whole area and on the acquisition of more information on mantle processes beneath the northern part of the Red Sea.

7 Conclusions

A large dataset containing the P- and S-wave arrival times from regional earthquakes provided by the Egyptian National Seismological Network was used for a tomographic investigation of the crustal structure beneath the area of the Gulf of Aqaba and northern Red Sea. The main products of this work included 3D models of P- and S-seismic velocities within the crust and uppermost mantle for these regions. The model results have helped us to close the gap between the existing small-scale active source studies of the uppermost crust beneath the offshore areas of the Red Sea and Gulf of Aqaba and large-scale regional mantle models beneath Africa and Arabia derived from the inversion of body and surface wave data.

The new seismic models revealed a strong high-velocity anomaly in the northern Red Sea, with sharp boundaries coinciding with the coastal line. This may be indicative of an oceanic or transitional (mafic-dominated) type of crust and seems to oppose the concept of gradual stretching of the continental crust in the northern Red Sea that has been proposed by some authors. However, the question about the development of the oceanic crust, specifically in regard to the absence of any traces

of ridges and spreading centers in the northern Red Sea that would require a rather dispersed extension of oceanic crust as opposed to spreading localized along rifts, still remains unanswered.

As was demonstrated in synthetic test results shown in Fig. 7, the absolute velocities in vertical sections can be used for estimating the variations of the Moho depth. According to our results, the Moho depth varies from ~20 km beneath the Red Sea to ~40 km beneath the Arabian Plate. In this sense, the crust in the Red Sea is not "classically" oceanic with a typical thickness of ~7 km. At the same time, strong high-velocity anomalies presume that the mafic component prevails here; thus, it cannot be associated with stretching of the continental crust.

In the middle and lower crust, the seismic anomalies seem to delineate a step-shaped pattern, which is indicative of the left-lateral displacement of the crust along the Dead Sea Transform fault. The estimated value of this displacement from the seismic tomography model is approximately 100 km; this is consistent with existing estimates from geological and geomorphology data for the southern part of the DST.

At the 40 km depth, no apparent link between the locations of seismic anomalies and the DST fault zone was observed. Previous studies also did not reveal any fault related structures in the uppermost mantle. This might indicate that the displacement along the DST occurs merely in the crust and decays with depth rapidly. However, this question still requires further investigations.

Acknowledgments. Earthquake data for this study were obtained from the Egyptian National Seismological Network. IK was supported by the Russian Science Foundation (grant #14-17-00430). The authors extend their appreciation to the Deanship of Scientific Research at King Saud University for funding the work through the research group project RG-1435-027. AP was supported by the German Research Foundation (DFG grant PE 2167/1-1).

Table 1. Values of some parameters used to calculate the main tomographic model.

Parameter description	Value
Grid spacing, horizontal	10 km
Minimum grid spacing, vertical	3 km
Minimum number of picks per event	6
Maximum residual deviation, P and S	1.5 s and 2 s
Smoothing for the P-velocity	1.5
Smoothing for the S-velocity	3
Station corrections, P and S	0.1 and 0.3
Weight for the source coordinate correction	5
Weight for the source origin time correction	5

Table 2. The optimal 1D P-velocity distribution used as a reference model for the tomographic inversion.

Depth, km	P-velocity, km/s
-3	4.9
10	6.0
20	6.7
30	7.5
50	8.0
100	8.2

Figure captions

Figure 1. A. Major tectonic framework of the study area schematically representing the main displacements of the major plates. The blue line is the transform fault, the red lines are the divergent areas, and the violet lines depict the convergent boundaries. DST is the Dead Sea Transform fault. B. Tectonic units in the area of the Gulf of Aqaba. Gray lines are faults in Egypt (Darwish and El Ababy, 1993; Bosworth and McClay, 2001); blue lines are faults in Saudi Arabia, and red dotted lines are dykes according to Eyal et al. (1981).

Figure 2. Distributions of seismic stations from the ENSN catalog (blue triangles) and ISC catalog (red triangles). Map at the regional scale (left plot) and within the study area (right plot). Orange dots represent the following types of seismicity: all events collected from the ENSN catalog (left) and selected relocated events used in this study (right).

Figure 3. P- and S-wave travel times versus the epicentral distance. P-wave travel times are indicated in blue and S-wave travel times in red. The dataset was from the initial catalog used as input for this study.

Figure 4. Distributions of the ray paths (gray dots) and nodes of the parameterization grid (red dots). Depth intervals and types of data are indicated on the top left of the maps.

Figure 5. Results of the checkerboard test with the model unchanged with depth for P- and S-velocity anomalies. The recovered velocity anomalies are presented in four depth sections. Dotted lines indicate the configurations of the "true" synthetic patterns. Triangles depict seismic stations.

Figure 6. Checkerboard tests with the model changing the sign of anomalies at 20 km depth. Here, only P-velocity anomalies are shown. Locations of the sections are shown in Fig. 2. Thin black lines indicate the configurations of the "true" synthetic patterns. Dots depict projections of seismic events located at the vicinity of the profile.

Figure 7. Synthetic test on recovering the Moho depth variations in section 2 (see Fig. 2 for the location of the profile). Upper plot is the synthetic model; middle and lower plots are the reconstruction results for the P- and S-velocities, respectively. Dotted line depicts the synthetic Moho interface, and dots depict the earthquakes used for inversion.

Figure 8. P- and S-anomalies resulting from the observed data inversion in four horizontal sections. At 10 km depth, major tectonic units (the same as in Fig. 1b) are shown. In sections at 20 and 30 km depth, the reference lines marking the displacements along the DST are depicted with green dotted lines.

Figure 9. Absolute P-velocity at 30 km depth and in four vertical sections. Locations of the sections are shown in the map. White dots are the projections of earthquakes onto the profiles.

Figure 10. Same as Fig. 7, but for the S-absolute velocities.

Figure 11. Back-reconstruction of the displacements along the DST since the initiation in the early Miocene (left) (Eyal et al., 1981) and present topography along the DST. Red lines mark the main structures at the initial stage for reference.

Figure 12. Back-reconstruction of the P-velocity model at 10 km and 30 km depth according to the DST displacements presented in Fig. 2. Green dotted lines depict the reference markers for the displacement. Violet lines are the structures discussed in the text. The red dotted lines are dykes according to Eyal et al. (1981).

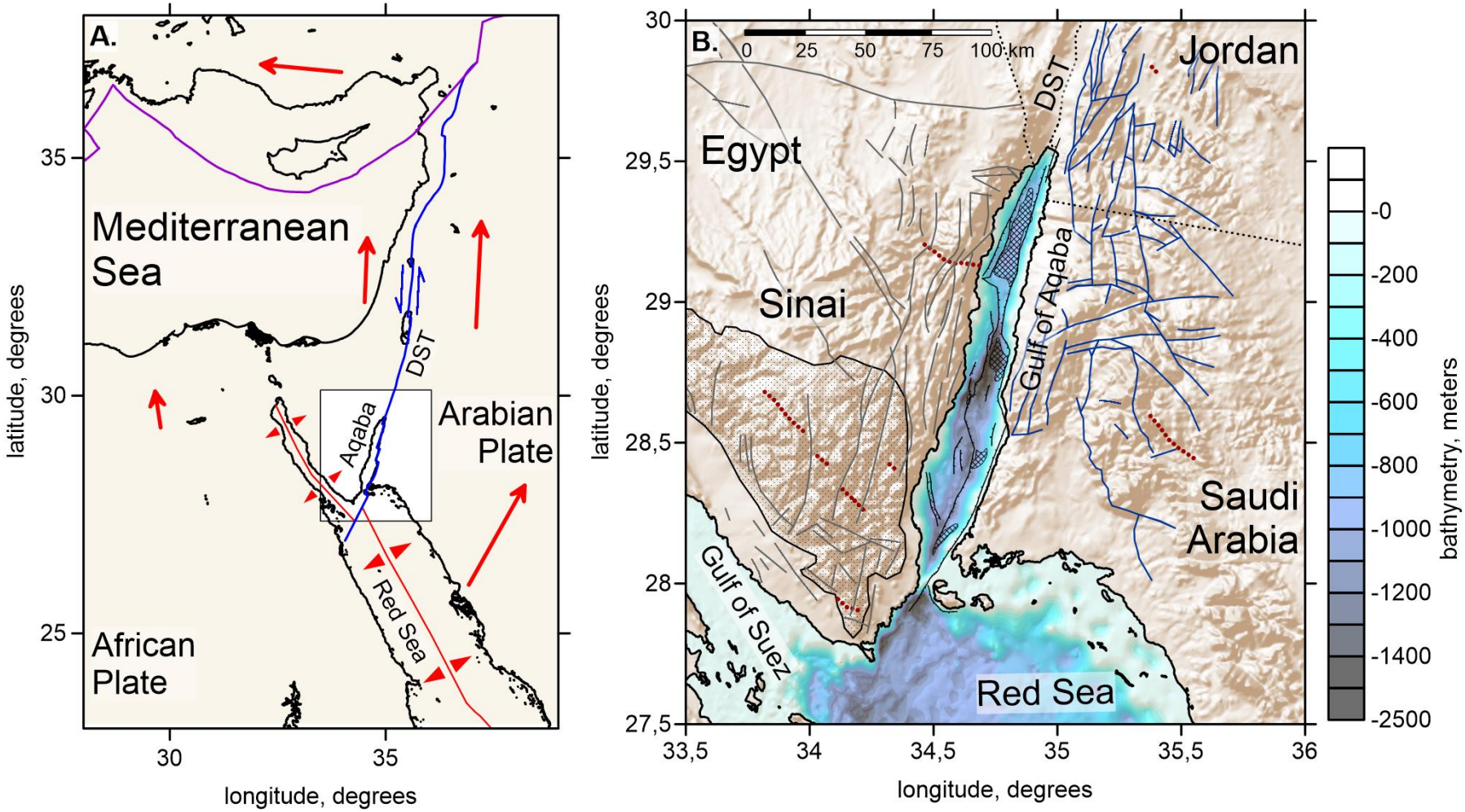

Figure 1. A. Major tectonic framework of the study area schematically representing the main displacements of the major plates. The blue line is the transform fault, the red lines are the divergent areas, and the violet lines depict the convergent boundaries. DST is the Dead Sea Transform fault. B. Tectonic units in the area of the Gulf of Aqaba. Gray lines are faults in Egypt (Darwish and El Ababy, 1993; Bosworth and McClay, 2001); blue lines are faults in Saudi Arabia, and red dotted lines are dykes according to Eyal et al. (1981).

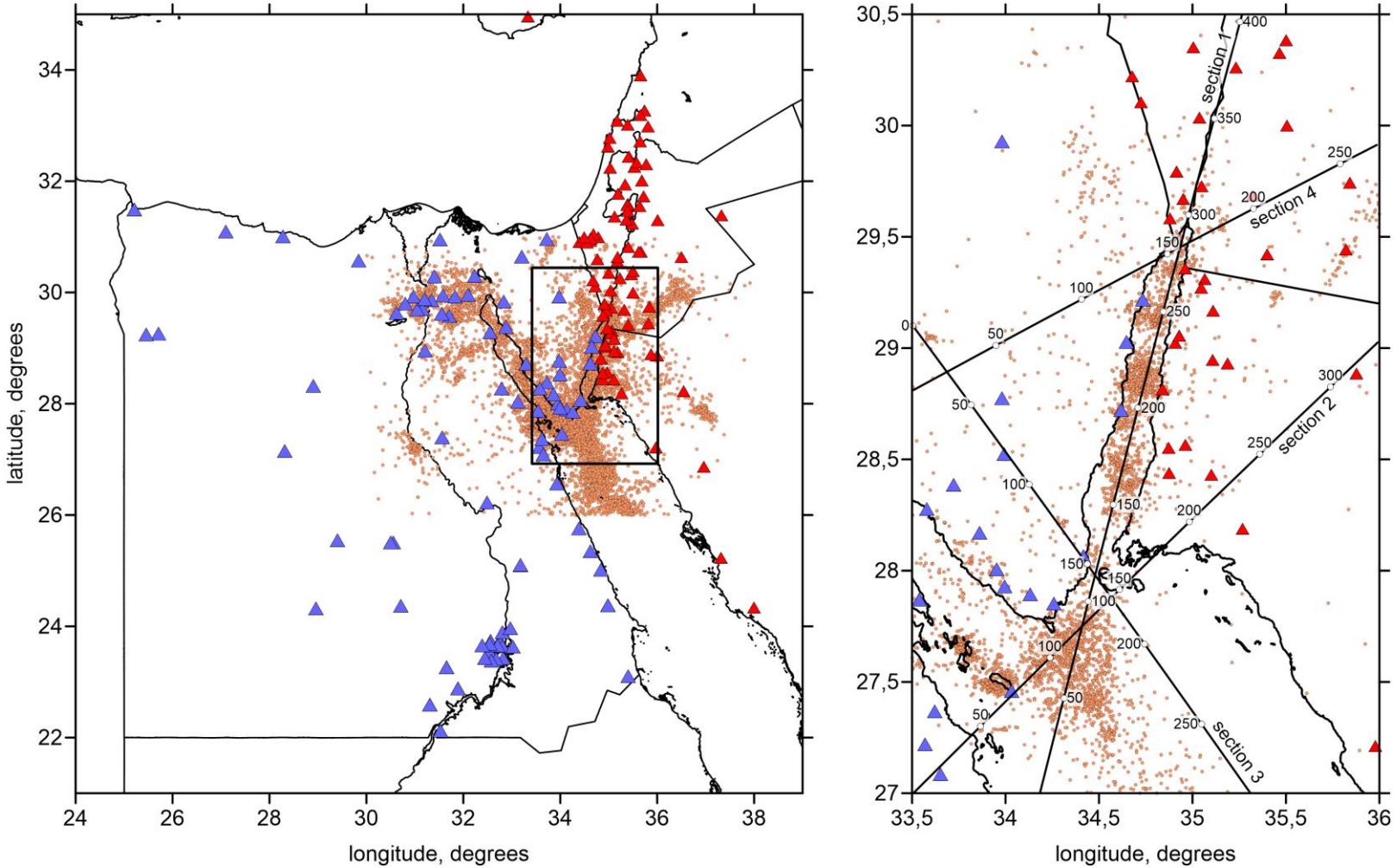

Figure 2. Distributions of seismic stations from the ENSN catalog (blue triangles) and ISC catalog (red triangles). Map at the regional scale (left plot) and within the study area (right plot). Orange dots represent the following types of seismicity: all events collected from the ENSN catalog (left) and selected relocated events used in this study (right).

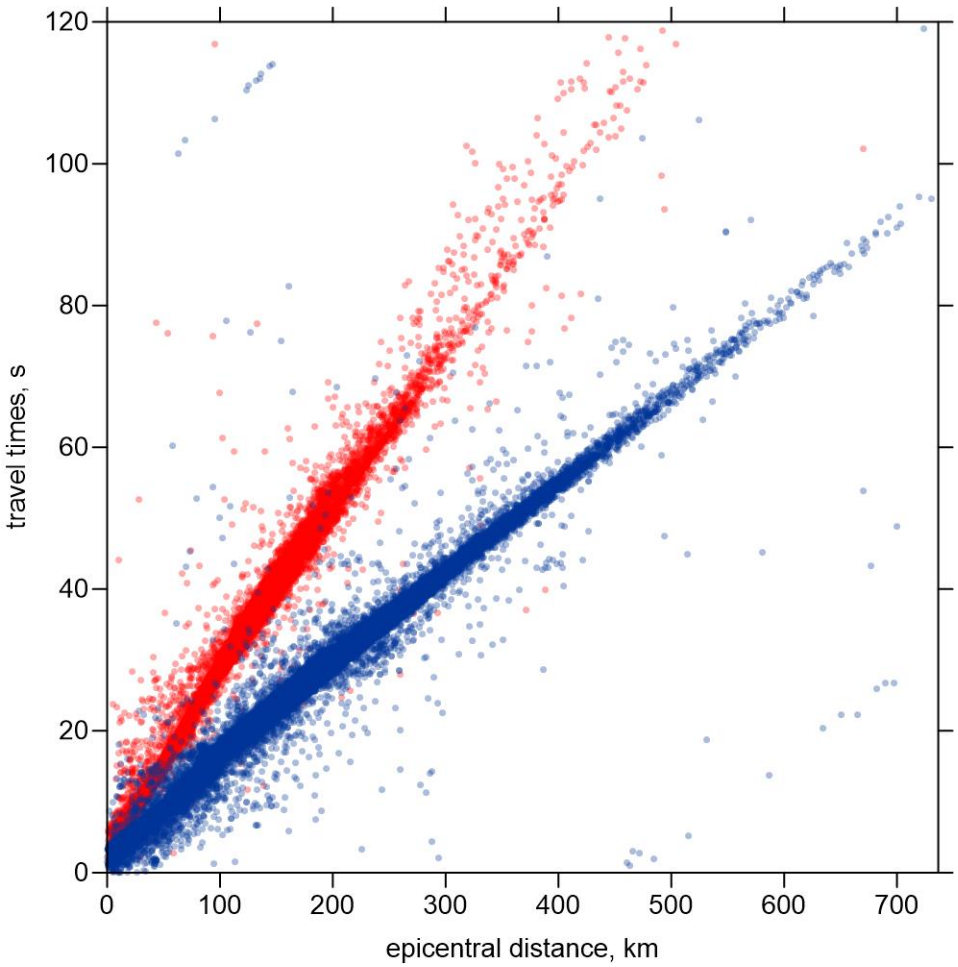

Figure 3. P- and S-wave travel times versus the epicentral distance. P-wave travel times are indicated in blue and S-wave travel times in red. The dataset was from the initial catalog used as input for this study.

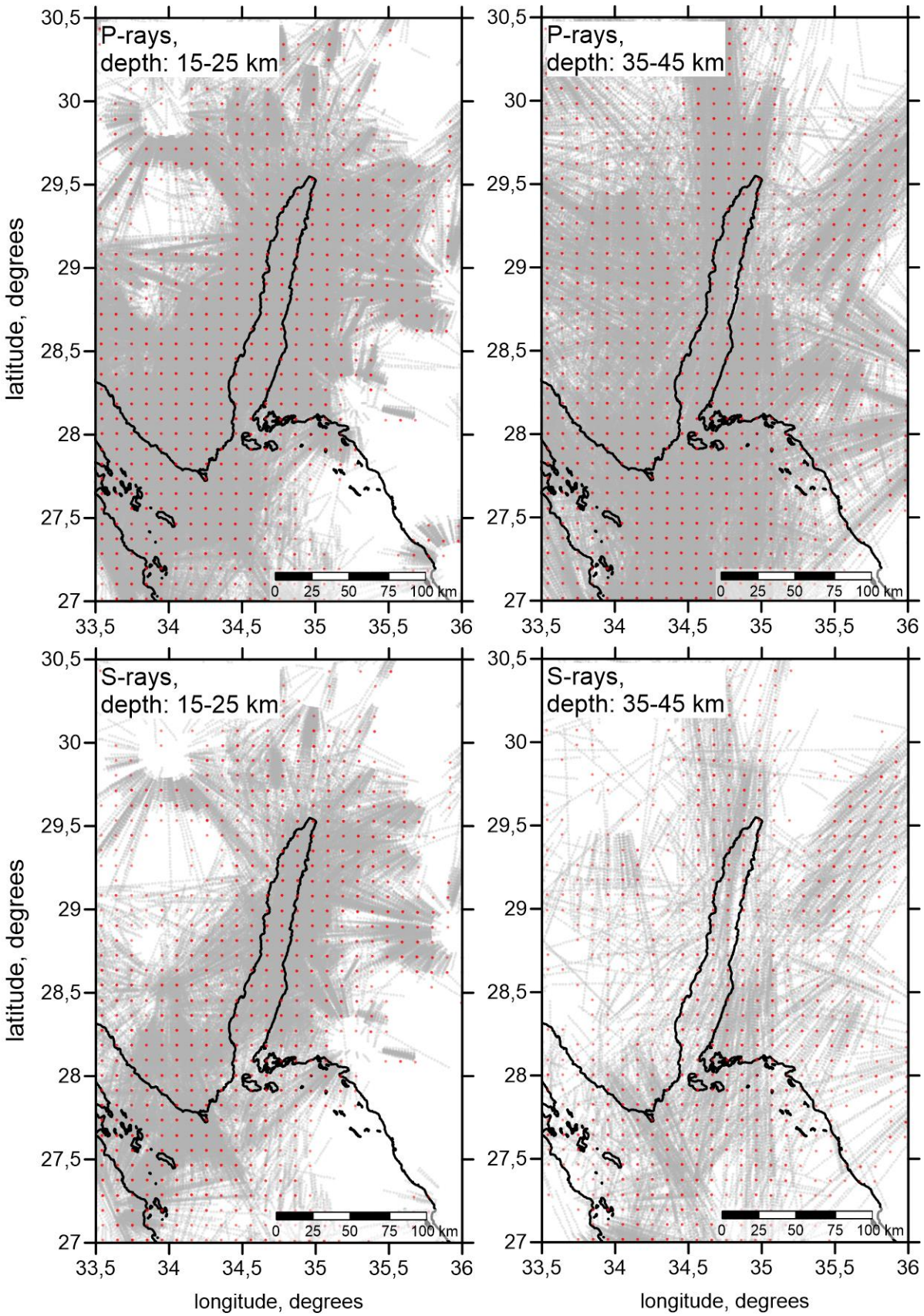

Figure 4. Distributions of the ray paths (gray dots) and nodes of the parameterization grid (red dots). Depth intervals and types of data are indicated on the top left of the maps.

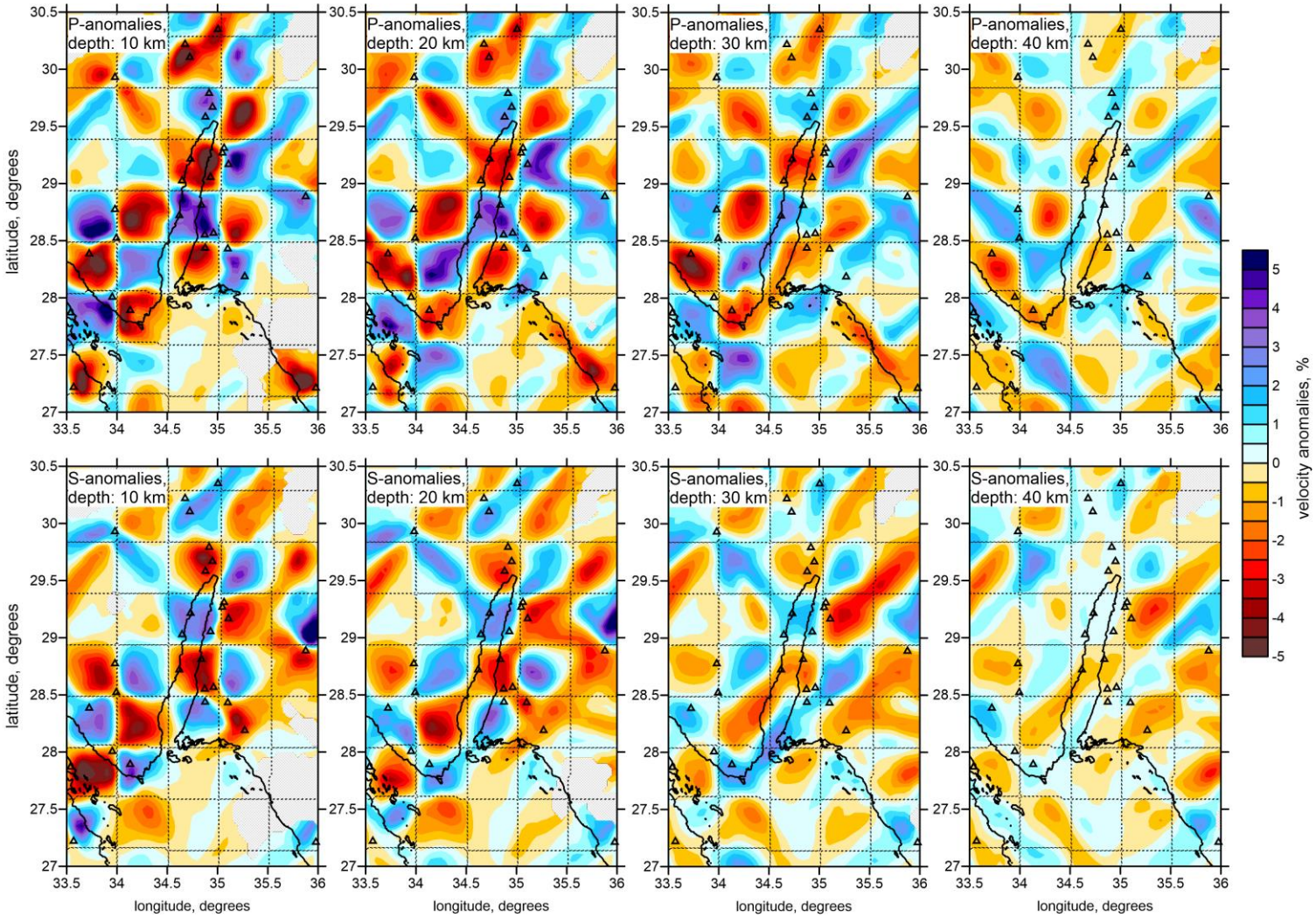

Figure 5. Results of the checkerboard test with the model unchanged with depth for P- and S-velocity anomalies. The recovered velocity anomalies are presented in four depth sections. Dotted lines indicate the configurations of the "true" synthetic patterns. Triangles depict seismic stations.

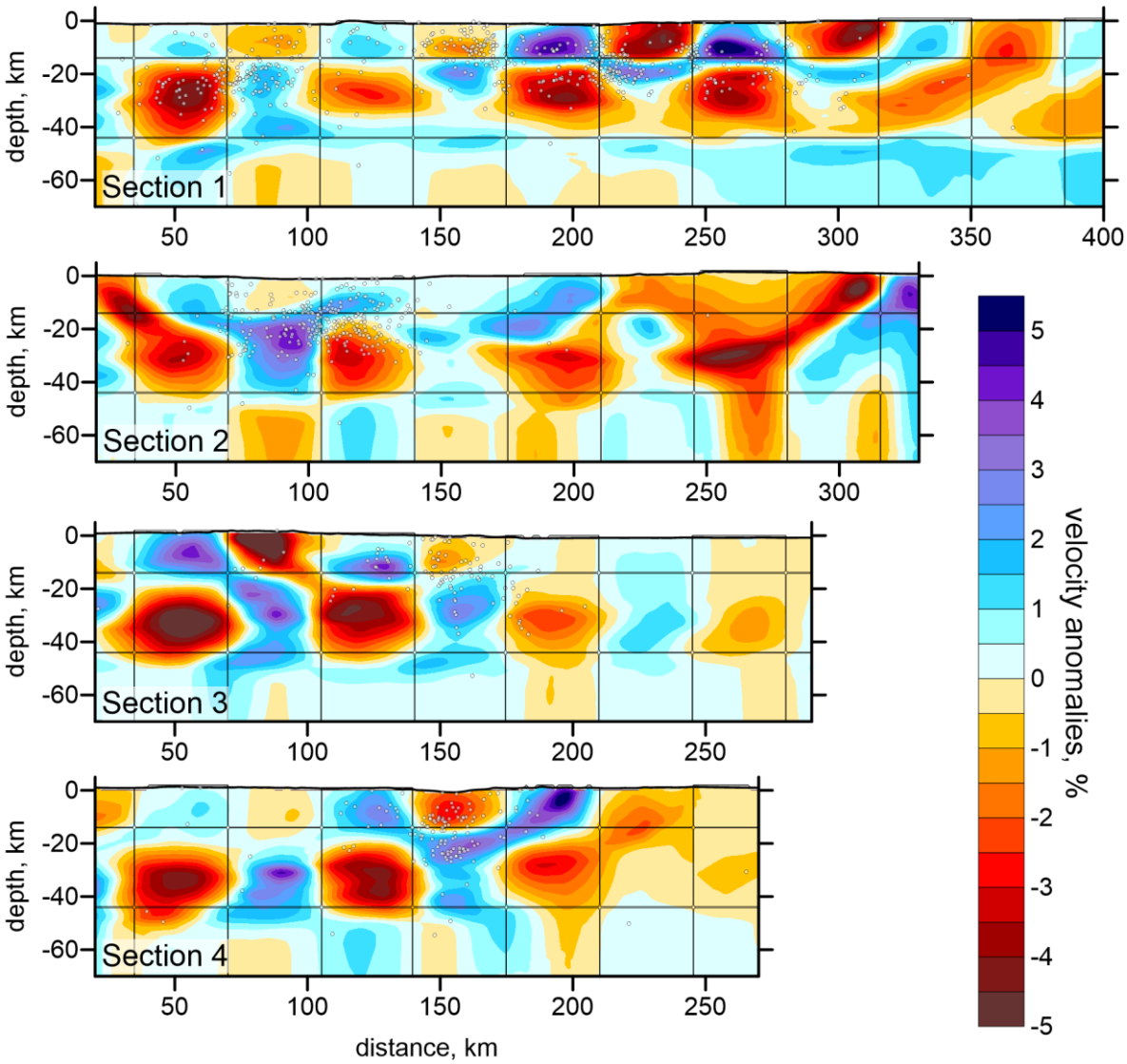

Figure 6. Checkerboard tests with the model changing the sign of anomalies at 20 km depth. Here, only P-velocity anomalies are shown. Locations of the sections are shown in Fig. 2. Thin black lines indicate the configurations of the "true" synthetic patterns. Dots depict projections of seismic events located at the vicinity of the profile.

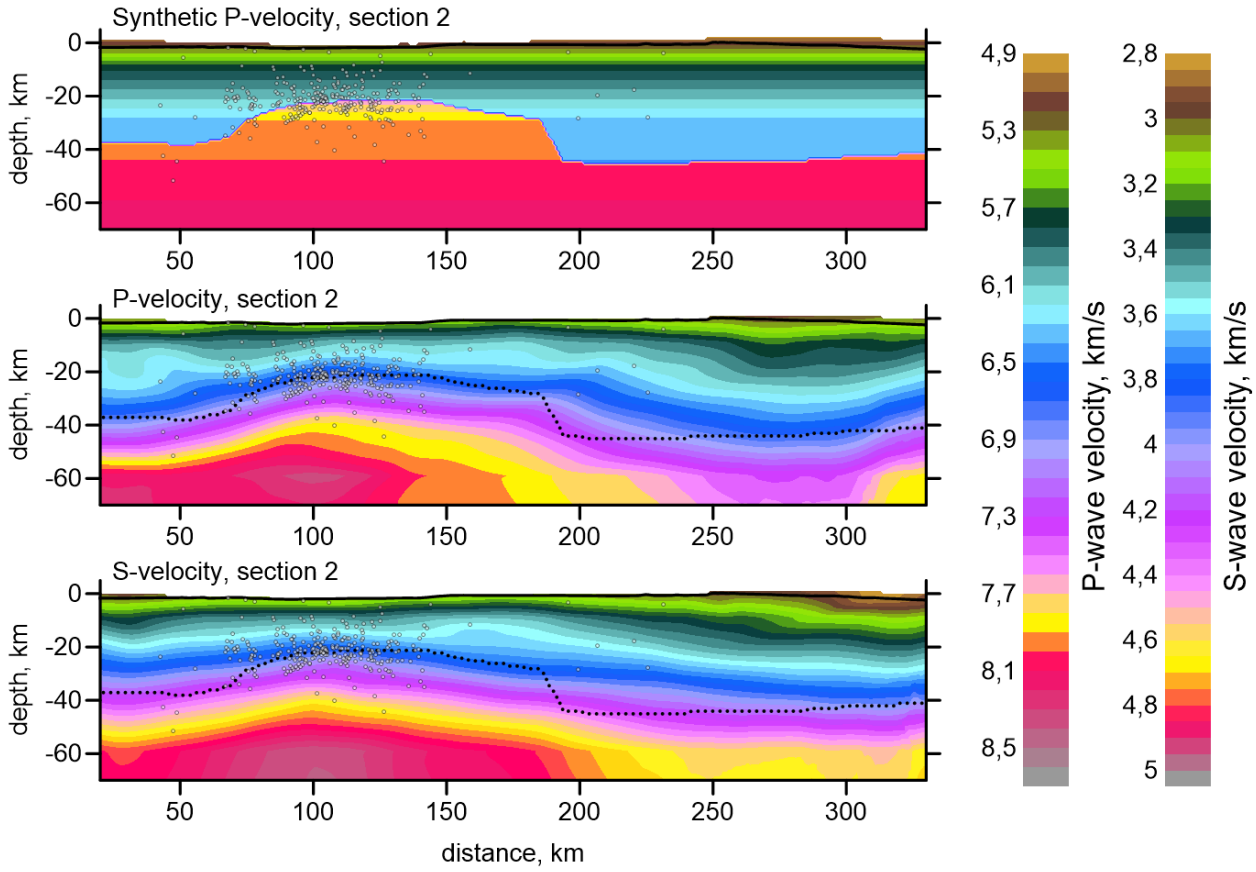

Figure 7. Synthetic test on recovering the Moho depth variations in section 2 (see Fig. 2 for the location of the profile). Upper plot is the synthetic model; middle and lower plots are the reconstruction results for the P- and S-velocities, respectively. Dotted line depicts the synthetic Moho interface, and dots depict the earthquakes used for inversion.

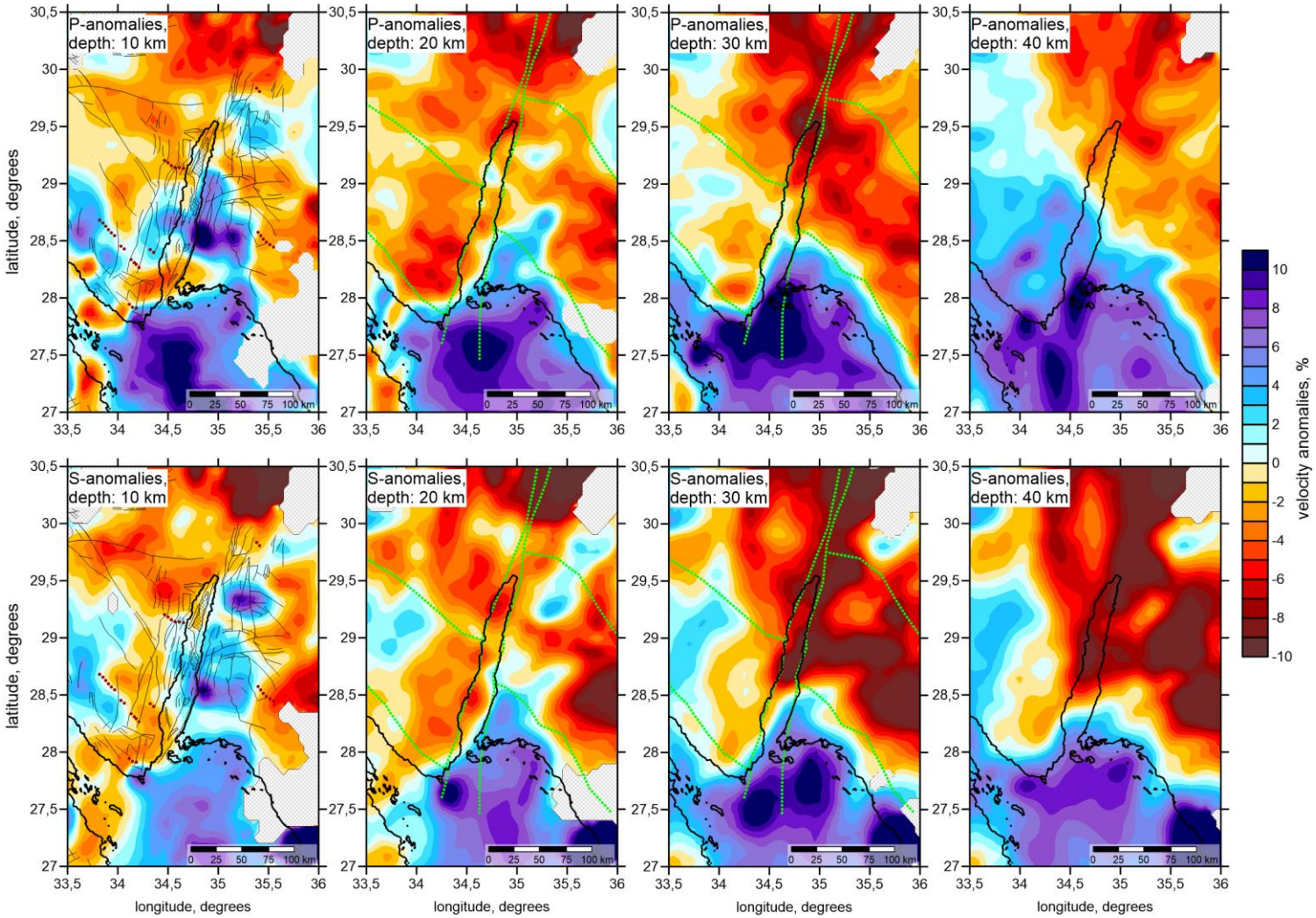

Figure 8. P- and S-anomalies resulting from the observed data inversion in four horizontal sections. At 10 km depth, major tectonic units (the same as in Fig. 1b) are shown. In sections at 20 and 30 km depth, the reference lines marking the displacements along the DST are depicted with green dotted lines.

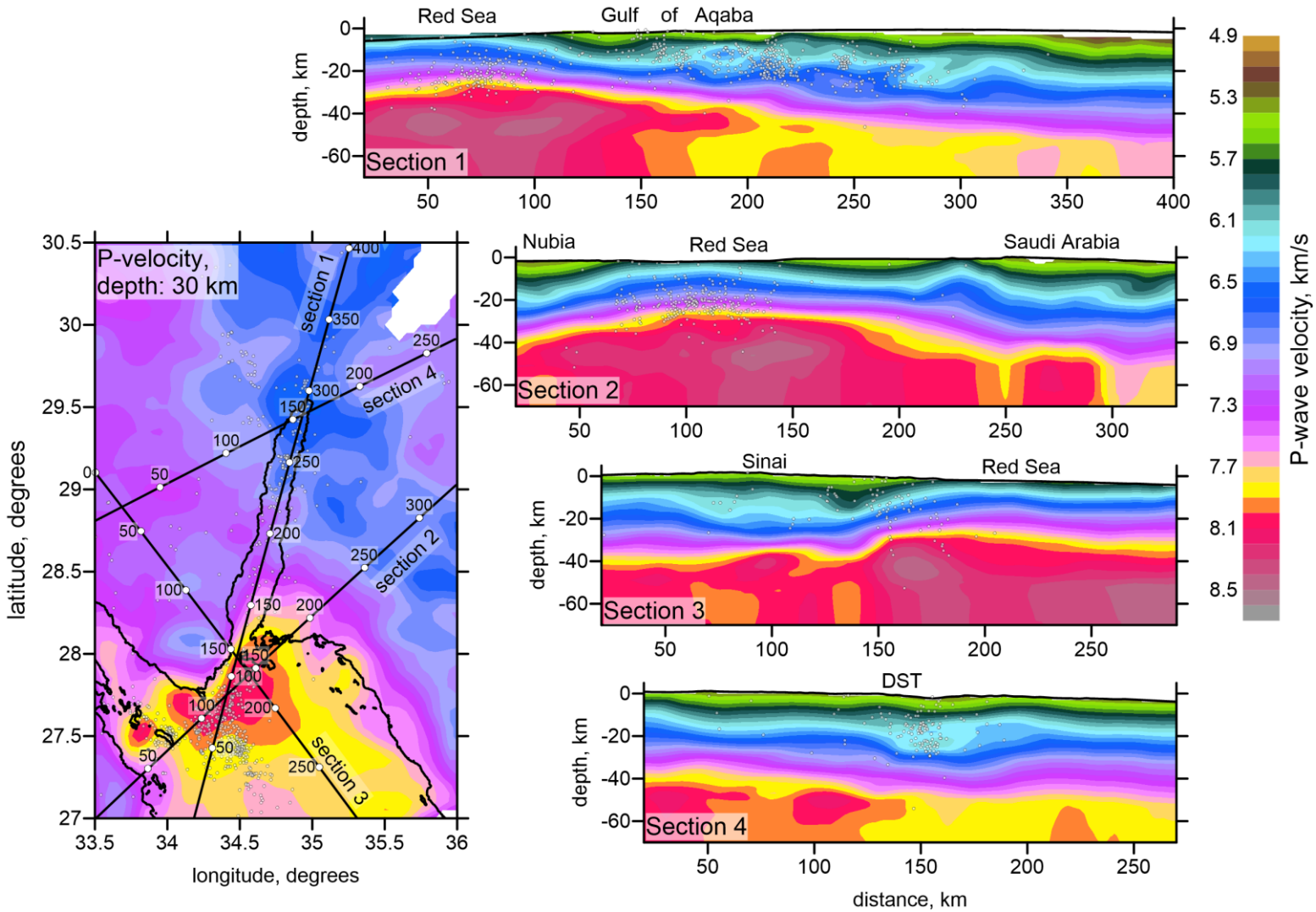

Figure 9. Absolute P-velocity at 30 km depth and in four vertical sections. Locations of the sections are shown in the map. White dots are the projections of earthquakes onto the profiles.

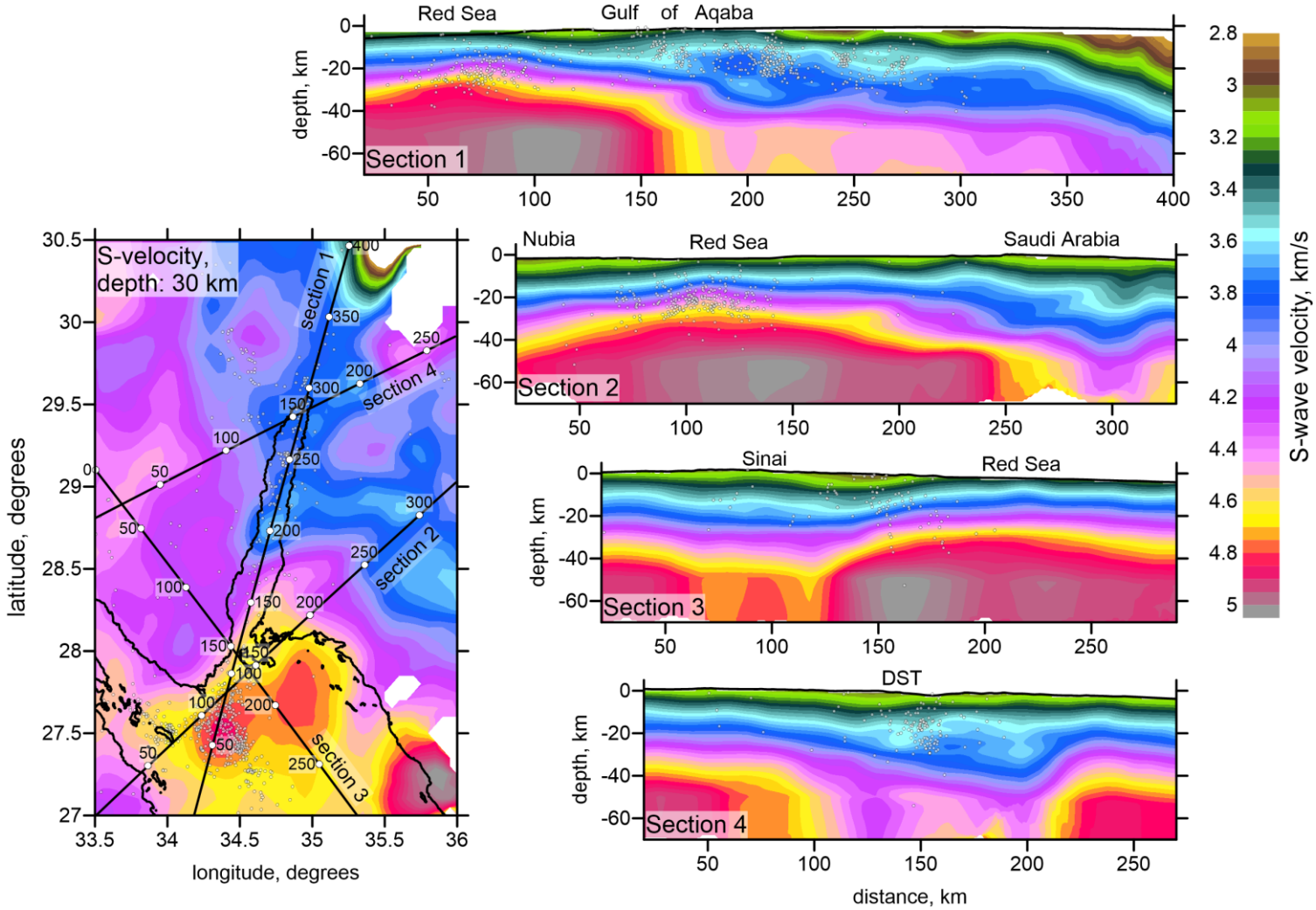

Figure 10. Same as Fig. 7, but for the S-absolute velocities.

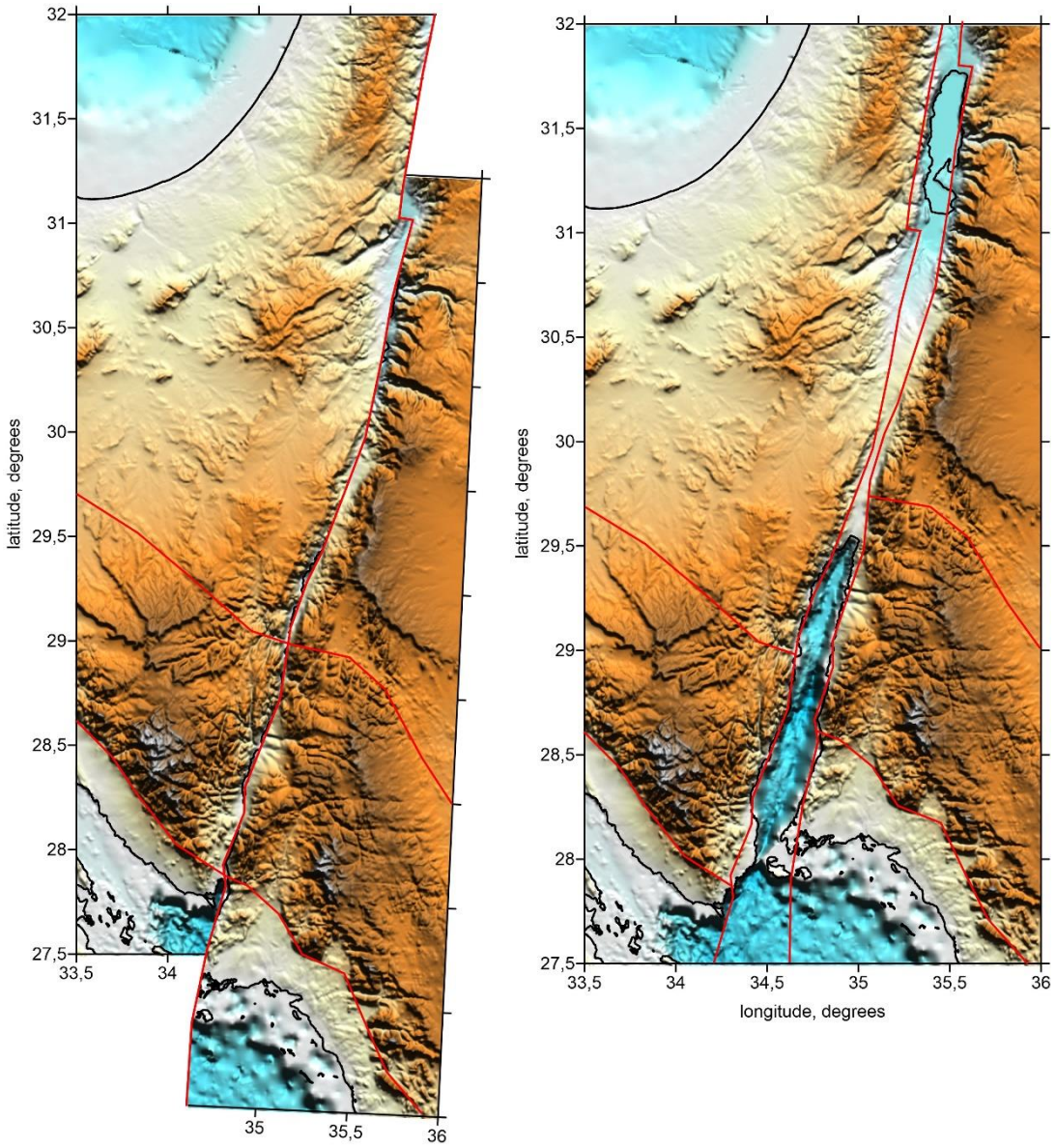

Figure 11. Back-reconstruction of the displacements along the DST since the initiation in the early Miocene (left) (Eyal et al., 1981) and present topography along the DST. Red lines mark the main structures at the initial stage for reference.

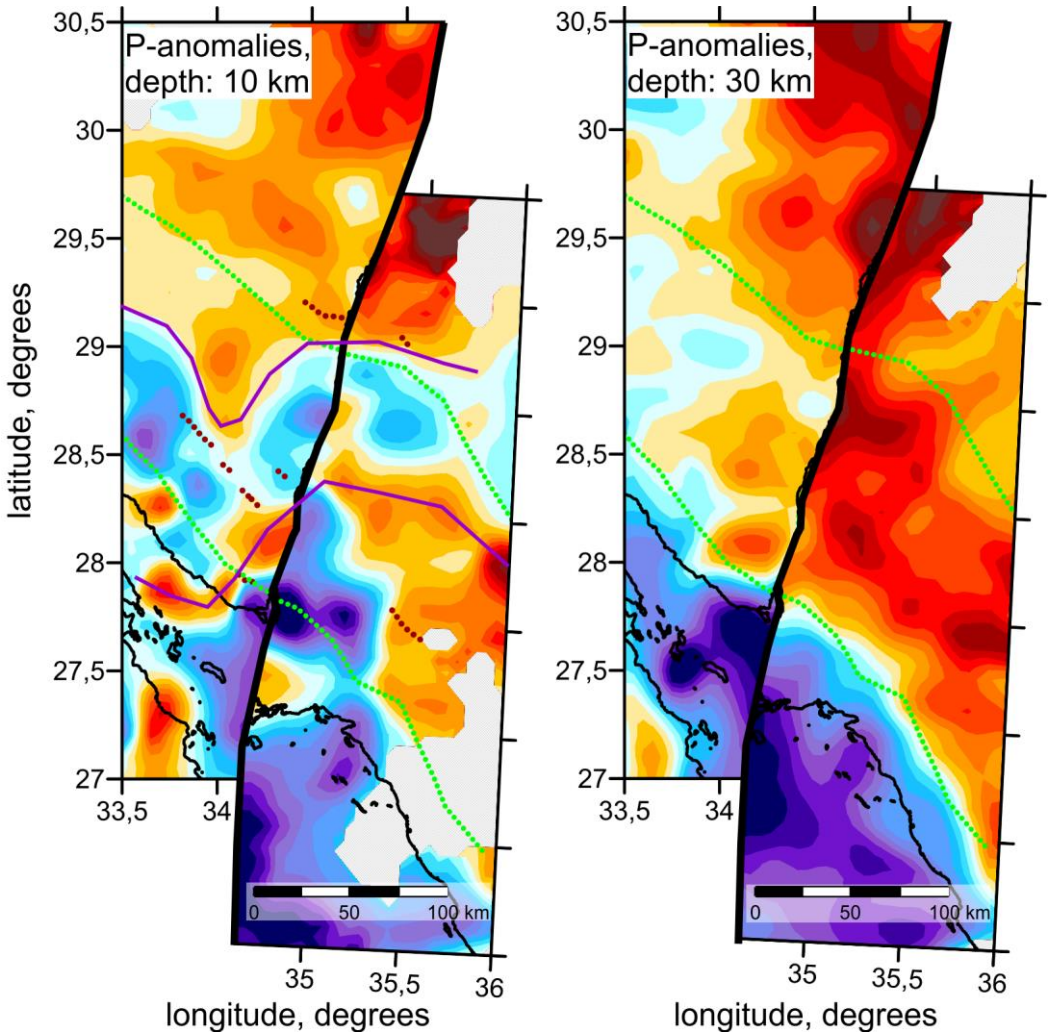

Figure 12. Back-reconstruction of the P-velocity model at 10 km and 30 km depth according to the DST displacements presented in Fig. 2. Green dotted lines depict the reference markers for the displacement. Violet lines are the structures discussed in the text. The red dotted lines are dykes according to Eyal et al. (1981).